JAERI-Research
2002-029

NUCLEAR DATA EVALUATION FOR ^{238}Pu, ^{239}Pu, ^{240}Pu, ^{241}Pu AND ^{242}Pu IRRADIATED BY NEUTRONS AND PROTONS AT THE ENERGIES UP TO 250 MeV

December 2002

A. Yu. Konobeyev, Tokio FUKAHORI and Osamu IWAMOTO

日本原子力研究所
Japan Atomic Energy Research Institute

本レポートは，日本原子力研究所が不定期に公刊している研究報告書です。
入手の問合わせは，日本原子力研究所研究情報部研究情報課（〒319-1195　茨城県那珂郡東海村）あて，お申し越しください。なお，このほかに財団法人原子力弘済会資料センター（〒319-1195　茨城県那珂郡東海村日本原子力研究所内）で複写による実費頒布をおこなっております。

This report is issued irregularly.
Inquiries about availability of the reports should be addressed to Research Information Division, Department of Intellectual Resources, Japan Atomic Energy Research Institute, Tokai-mura, Naka-gun, Ibaraki-ken, 319-1195, Japan.

編集兼発行　　日本原子力研究所

JAERI-Research 2002-029

Nuclear Data Evaluation for ^{238}Pu, ^{239}Pu, ^{240}Pu, ^{241}Pu and ^{242}Pu Irradiated by Neutrons and Protons at the Energies up to 250 MeV

A. Yu. Konobeyev, Tokio FUKAHORI and Osamu IWAMOTO

Department of Nuclear Energy System

Tokai Research Establishment

Japan Atomic Energy Research Institute

Tokai-mura, Naka-gun, Ibaraki-ken

(Received October 9, 2002)

The evaluation of nuclear data for plutonium isotopes with atomic mass number from 238 to 242 has been performed. Neutron data were obtained at the energies from 20 to 250 MeV and combined with JENDL-3.3 data at 20 MeV. Evaluation of the proton data has been done from 1 to 250 MeV. The coupled channel optical model was used to obtain angular distributions for elastic and inelastic scattering and transmission coefficients. Pre-equilibrium exciton model and Hauser-Feshbach statistical model were used to describe neutron and charged particles emission from the excited nuclei. These evaluation is the first work for producing the full set of evaluated file up to 250 MeV for plutonium isotopes.

Keywords: Nuclear Data, Evaluation, Intermediate Energy, Neutron, Proton, Cross Section, Fission, Pre-equilibrium Model, Statistical Model, ^{238}Pu, ^{239}Pu, ^{240}Pu, ^{241}Pu, ^{242}Pu

^{238}Pu, ^{239}Pu, ^{240}Pu, ^{241}Pu, ^{242}Pu に対する 250 MeV までの中性子及び陽子入射核データの評価

日本原子力研究所東海研究所エネルギーシステム研究部
A.Yu. Konobeyev・深堀　智生・岩本　修

(2002年10月9日受理)

質量数238から242までのプルトニウム同位体に対する核データの評価を行った。中性子データは20から250 MeVまで評価を行い、20 MeVでJENDL-3.3とつなげた。陽子データの評価は1から250 MeVまで行った。チャンネル結合光学モデルを用い、弾性散乱、非弾性散乱の角度分布及び透過係数を求めた。前平衡過程の励起子モデルとHauser-Feshbachの統計モデルにより、励起原子核からの中性子及び荷電粒子の放出を求めた。本評価は250MeVまでのプルトニウム同位体に対する評価済ファイル作成として、初めてのものである。

東海研究所：〒319-1195 茨城県那珂郡東海村白方白根2-4

Contents

目　次

This is a blank page.

1. Introduction

Plutonium is considered now as the principal component of nuclear fuel in different ADS concepts. Plutonium isotopes with atomic mass number A=238-242 have the primary importance from this point of view. The goal of this work was to obtain the nuclear data for plutonium isotopes suitable to study neutron transport, heating, change of nuclide composition of the nuclear fuel and for other applications in the whole energy range from thermal energy up to 250 MeV.

Both neutrons and protons are considered as the incident particles in the present work. The evaluation has been done with theoretical models and semi-empirical and empirical approaches, whose validity has been approved based on the big number of experimental data. Neutron data at the energy 20 MeV were combined with new JENDL-3.3 evaluation [1-4]. Proton data are obtained from 1 to 250 MeV.

2. Nuclear Models Used for the Calculation of Reaction Characteristics

The description of the nuclear model and codes used in the present work is given in Ref.[5]. The coupled-channel optical model realized in the ECIS96 code [6] has been used to obtain total cross section, angular distributions for elastic and inelastic scattering for neutrons and protons, to calculate the transmission coefficients for neutrons and charged particles. The Hauser-Feshbach statistical model and the pre-equilibrium exciton model were used to calculate particle emission spectra and nuclide yields. GNASH code [7] was applied for the numerical calculations.

Nuclear level density was calculated with generalized superfluid model [8,9]. The description of the fission barriers includes the consideration of the spin and the temperature effects as described in Ref.[5]. Exciton model based on the solving of master equations has been used for the calculation of pre-equilibrium nucleon spectra. Exciton transition rates and particle-hole level density has been calculated taking into account the final depth of the potential well and surface effects according to Ref.[10]. The models used for the calculation of the complex particle pre-compound spectra are described in Ref.[5].

The multiple pre-compound emission has been considered. Certain improvement in the description of such emission has been done in the present work comparing with GNASH algorithm [7] and Ref.[5].

The general expression for the second pre-equilibrium particle emission spectra calculation used in GNASH code has the following form [11]

$$\frac{d\sigma_j^{mpe}}{dE}=\sum_n\sum_{i=\pi,\upsilon}\int_{U=E+Q}^{U_{max}}\frac{d\sigma_i^{(n)}}{dU}\left(\frac{\omega(1p,0,E+Q)\,\omega(p-1,h,U-E-Q)}{p\;\omega(p,h,U)}R_{i,j}^{(n)}\right)T_j(E)\,dU \qquad (1)$$

where "i" and "j" is the type of the first and second pre-compound particle emitted, respectively; E is the emission energy and Q is the separation energy for "j"-particle; $d\sigma^{(n)}{}_i/dU$ is the differential transition cross section of p-h state in the n-exciton number after pre-equilibrium emission of "i"-particle; $R^{(n)}{}_{i,j}$ is the neutron-proton distinguishability factor calculated according to Ref.[12]; $T_j(E)$ is the probability of the "j"-particle to escape with energy E; summing is for all "n"-exciton states and primary particle types.

The calculation of $T_j(E)$ from Eq.(1) in GNASH code [7] is based on the simple approximation considering the s-wave transmission coefficient. The actual values used in the code are shown in Fig.1. In the present work the probability of the particle emission $T_j(E)$ is calculated as follows

$$T_j(E)=\frac{\lambda_j^e(E)}{\lambda_j^e(E)+\lambda_j^+(E+Q)}, \qquad (2)$$

where λ^e_j is the particle emission rate and λ^+_j is the intranuclear transition rate corresponding to the absorption of "j"-particle in nucleus.

The emission and intranuclear transition rates are calculated according to the following relations

$$\lambda_j^e=\frac{(2S_j+1)\mu_j E\sigma_j^{inv}(E)}{\pi^2\hbar^3 g_j}, \qquad (3)$$

$$\lambda_j^+=V_j\,\sigma_j^{nn}(E+Q)\rho, \qquad (4)$$

where S_j and μ_j are the spin and the reduced mass of "j"-particle, $\sigma^{inv}{}_j$, is the inverse reaction cross section, g_j is the single particle level density, V_j is the velocity of the particle of "j"-type inside the nucleus, $\sigma^{nn}{}_j$ is the nucleon-nucleon interaction cross section corrected for the Pauli principle, ρ is the nuclear density.

Calculation of $T_j(E)$ according to Eqs.(2)-(4) corresponds to the basic assumptions of the hybrid exciton model [12,13]. The values of $T_j(E)$ calculated in such a way are shown in Fig.1 for neutrons and protons. An example of particle spectra calculated with the $T_j(E)$ values obtained by Eqs.(2)-(4) is shown in Fig.2 for ^{209}Bi(p,p') reaction at the incident proton energy equal to 62 MeV. The experimental data are taken from Ref.[14]. The use of Eqs.(2)-(4) improves the agreement with the experimental data as shown in Fig.2.

Fission neutron, charged particle and γ-spectra were calculated with approach from Ref.[15] using ALICE/ASH (ALICE/IPPE) code [16,17] as described in Ref.[5].

3. Neutron Nuclear Data Evaluation

^{239}Pu

The total cross section calculated with ECIS96 code and the optical potential from Ref.[5] is shown in Fig.3 for ^{239}Pu together with the experimental data [18,19]. For the comparison the cross section obtained using the optical potential from Ref.[20] and Barashenkov systematics values [21,22] are shown. The present calculations are in agreement with the systematics prediction [21,22].

Figures 4and 5 show the elastic and reaction cross sections obtained in the present work, calculated using the optical potential [20] and estimated according to systematics of Barashenkov [21,22] and Fukahori [23]. In general the agreement is observed with the present evaluation and systematics. The goodness of fit varies with the neutron incident energy.

The obtained elastic scattering angular distribution at the neutron energy E_n = 20 MeV is shown in Fig.6 together with the data from JENDL-3.3, BROND-2 and CENDL-2 libraries. Data from ENDF/B-VI are not shown, they nearly coincide with JENDL-3.3 data. There is a reasonable agreement between the calculation and JENDL-3.3 data. This agreement is the most important in the range of two first scattering peaks playing the significant role in the interaction of neutrons with media.

The other comparison is made with the data from Refs.[24,25] obtained for ^{239}Pu at the energies up to 50 MeV. The calculated elastic angular distribution are shown together with the evaluation from Refs.[24,25] in Fig.7 at the incident neutron energies equal to 20 and 50 MeV. The data are close at the scattering angles below 30^0.

The direct inelastic scattering cross sections were calculated for the seven members of the ground state rotational band: $3/2^+$ (7.86 keV), $5/2^+$ (57.28 keV), $7/2^+$ (75.71 keV), $9/2^+$ (163.76 keV), $11/2^+$ (194 keV), $13/2^+$ (317 keV) and $15/2^+$ (360 keV) levels. Fig.8 shows the calculated direct inelastic scattering cross sections at the energies up to 250 MeV.

The relative contribution of different nuclei in the fission cross section for ^{239}Pu is shown in Fig.9. The fission of plutonium and neptunium isotopes provides more than 80 % of the (n,f) cross section for the whole energy range up to 250 MeV. The contribution of isotopes with Z=94 drops from 100 % at low energies to 50 % at 130 MeV and to 31 % at 250 MeV. The similar features are for other plutonium isotopes interacting with neutrons considered in the present work. The contributions to the fission cross section of isotopes with Z=94, Z=93 and Z=92 are shown for ^{239}Pu, ^{240}Pu, ^{241}Pu, ^{242}Pu at the different neutron energies in Tables 1-3.

The fission cross section calculated with help of GNASH code is shown in Fig.10 together with the measured data from Refs.[26-29]. Also the values obtained using ALICE/ASH code, the cross sections predicted by the systematics [23] and evaluated in Ref.[30] are presented. The cross sections calculated by GNASH code at the energy above 50 MeV are close to the latest experimental results [29] obtained and to

the values evaluated in Ref.[30]. The final evaluated data for (n,f) reaction cross section were obtained based on GNASH code calculations and on the analysis of the available experimental data.

The neutron production cross section and the contribution of the pre-fission emission calculated by GNASH code are shown in Fig.11. JENDL-3.3 data are also presented. The good agreement between calculated cross sections and ones taken from JENDL-3.3 is observed at the neutron energy equal to 20 MeV. One can see that at the energies above 20 MeV the neutrons are emitted mainly before the fission[1] and the (n,xnypzα) reactions plays the minor role in the neutron production.

The neutron and proton production cross section obtained with GNASH code are compared with ALICE/ASH code calculations in Fig.12. On the whole, there is a reasonable agreement between various code calculations. The values obtained using ALICE/ASH code for neutron yield are slightly overestimated comparing with GNASH results at the energies above 100 MeV. It should be noted that the absorption cross section is the same for both code calculations.

Figure 13 illustrates (n,xn) reaction cross sections for ^{239}Pu. Below 20 MeV JENDL-3.3 data are shown. The neutron emission from the isotopes with Z=94 and Z=93 producing during the nuclear reaction gives up to 78 % of total neutron production calculated by GNASH code. The contribution of Z=94 isotopes in the total neutron yields[2] falls from 100 % at the low energies, to 77 % at 100 MeV, to 50 % at 200 MeV and to 43 % at 250 MeV-neutron energy. At the same time the contribution of Z=94 isotopes in the total proton production declines slightly with the incident neutron energy growth and is equal to 90 % at 250 MeV.

The evaluated average number of prompt neutrons per fission <ν> is shown in Fig.14 together with the available experimental data above 20 MeV [31] and JENDL-3.3 data. ALICE/ASH code has been used to obtain the number of the post-fission neutrons. The pre-fission contribution was calculated using GNASH code.

Figure 15 illustrates the calculated normalized fission spectrum at the primary neutron energy equal to 250 MeV. For the sake of comparison the standard Maxwellian and Watt fission spectra are shown in the figure. The temperature Θ for the Maxwellian spectrum was defined from the calculated fission spectra maximum location.

$$f(E \to E') = exp(-E'/a)\,sinh(\sqrt{bE'})$$
$$\times\left[\frac{1}{2}\sqrt{\frac{\pi a^3 b}{4}}\,exp\left(\frac{ab}{4}\right)\left\{erf\left(\sqrt{\frac{E-U}{a}}-\sqrt{\frac{ab}{4}}\right)+erf\left(\sqrt{\frac{E-U}{a}}+\sqrt{\frac{ab}{4}}\right)\right\}-a\,exp\left\{-\left(\frac{E-U}{a}\right)\right\}sinh\left\{\sqrt{b(E-U)}\right\}\right]^{-1}$$

For the Watt spectrum, $f(E\to E')$, shown the values of a and b constants in above equation are equal to a=1.5, b=3x10^{-6}. The variation of these values cannot significantly improve the agreement between the

[1] The fission neutrons are not yet accounted for.

[2] See the comment above

shapes of the calculated distribution and the Watt spectrum at the outgoing neutron energies above 10 MeV. The data presented in Fig.15 show that the Maxwellian and Watt energy distributions underestimate considerably the high-energy tail of the fission spectrum.

Proton production cross section is compared in Fig.16 with the systematics value at 14.5 MeV [32], FENDL/A-2 data and the data measured in Ref.[33]. At the energy around 14.5 MeV the calculated values are in the good agreement with experimental data [33] and the cross sections from FENDL/A-2.

Calculated deuteron production cross section is shown in Fig.17 together with the cross sections predicted by the systematics at 14.5, 62, 90 and 160 MeV. The systematics value at 14.5 MeV was obtained in Ref.[32] and corrected to exclude the possible contribution of (n,np) reaction to the measured sums of (n,d) and (n,np) reactions cross sections.

Figures 18-20 show the evaluated triton, ^{3}He, α-production cross sections and the systematics predictions at the different incident energies. The total yields and the values corresponding to the particle emission before the fission and from (n,xnypzα) reactions are presented. The systematics value for (n,t) reactions at 14.6 MeV was obtained according to Ref.[34] and for (n,α) reaction at 14.5 MeV according to Ref.[35]. The existing systematics for (n,^{3}He) reaction cross section [32] is not used in the present work, it is based on the rather limited number of the available experimental data for this reaction. The systematics at 62, 90 and 160 MeV corresponds to the proton induced reactions. They were obtained in Ref.[5]. The cross sections predicted by the systematics [5,32,34,35] for the reactions considered are shown in Tables 4-7 for various plutonium isotopes.

Figure 21 presents the calculated charged particle yields from the excited fission fragments. The total γ-production cross section including the contributions from the γ-emission at the different reaction stages is shown in Fig.22 for ^{239}Pu in comparison with n+^{238}U interaction.

^{240}Pu

The calculated total cross section is shown in Fig.23 together with JENDL-3.3 data and systematics values [21,22]. A good agreement is observed with the cross section taken from JENDL-3.3 below 20 MeV, and also with one predicted by the systematics. The elastic and reaction cross sections obtained are presented in Figs.24 and 25 in comparison with the systematics [21-23] and JENDL-3.3 data.
Figure 26 illustrates the calculated direct inelastic scattering cross sections for three lowest levels of ^{240}Pu at the energies up to 250 MeV.

The fission cross sections calculated with GNASH code, ALICE/ASH code, estimated by the systematics [23] and measured in Refs.[28,36] are shown in Fig.27. It should be noted that GNASH code calculations are in a good agreement with JENDL-3.3 data below 20 MeV omitted in Fig.27. The final data evaluated for (n,f) reaction cross section are shown in Fig.28 and signed as "JENDL-HE". The maximal divergence between GNASH calculations and the evaluated (n,f) cross section does not exceed 7.8 %.

Neutron and proton production cross sections calculated with GNASH and ALICE/ASH codes are compared in Fig.29. Both cross sections calculated do not include the contribution from the post-fission events. Figure 30 shows the ratio of these cross sections calculated by ALICE/ASH code to the ones obtained by GNASH code. The observed difference between two set of the calculations is about 10 % for neutron production cross section at the energies above 25 MeV. For the proton yield the main divergence is below 40 MeV, at the energies above 60 MeV the difference is less than 5 %.

Figure 31 presents (n,xn) reaction cross sections for ^{240}Pu. The data are combined with JENDL-3.3 at the energy 20 MeV.

As with ^{239}Pu, the pre-fission emission for ^{240}Pu plays the main role in the neutron production at the energies above 20 MeV. The proportion of the post and pre-fission neutron yield is illustrated in Fig.32. Calculated total number of prompt fission neutrons is in a good agreement with JENDL-3.3 data at 20 MeV. The charged particle production cross sections are shown in Figs.33-37 together with the cross sections evaluated with systematics [5,32,34,35] and the data taken from FENDL/A-2. The calculated proton, triton and α-production cross sections are close to FENDL/A-2 data at the energies around 14.5 MeV. At the higher energies the reasonable agreement is observed for the calculated cross sections and ones predicted by the systematics [5].

^{238}Pu, ^{241}Pu, ^{242}Pu

For the considered plutonium isotopes the amount of the experimental data above 20 MeV is noticeably less than in the case of ^{239}Pu and ^{240}Pu. Noted above the general features of neutron interactions with the plutonium isotopes at the intermediate energies remain valid for ^{238}Pu, ^{241}Pu and ^{242}Pu.
The calculated total cross sections for the considered plutonium isotopes are shown in Figs.38-40 together with the experimental data [37] and the cross sections taken from JENDL-3.3. The systematics [21,22] is not valid in such case.

Figures 41-43 present the evaluated fission cross sections for ^{238}Pu, ^{241}Pu and ^{242}Pu isotopes and the measured data. The experimental data are taken from Ref.[38] for ^{241}Pu and from Refs.[28,36] for ^{242}Pu. The evaluated cross section for ^{241}Pu was obtained based on the results of GNASH code calculations. The additional small correction was made using the fission cross section ratio for ^{241}Pu and ^{240}Pu predicted by the systematics [23] and the evaluated (n,f) cross section for ^{240}Pu.

Figure 44 illustrates the neutron production cross sections for different plutonium isotopes above 20 MeV. The data shown correspond to the neutron emission preceding the fission and from (n,xnypzα) reactions.

The total neutron production cross section including contribution from post-fission events has the close values for all plutonium isotopes from ^{239}Pu to ^{242}Pu. The maximal difference for this value for various isotopes is 4.4 % at the incident neutron energy equal to 250 MeV.

4. Proton Nuclear Data Evaluation

The experimental data for the proton interactions with plutonium isotopes are rather scarce. It is necessary to note the incompleteness of EXFOR data comparing with the other compilations (e.g. [39-41]).

^{239}Pu

The calculated reaction cross section with coupled channel model and the optical potential from Ref.[5] is shown in Fig.45. Also, the result of the calculation with the optical potential from Ref.[20] and the cross section estimated by the systematics [21,22] are presented in Fig.45.

Figure 46 illustrates the elastic scattering angular distributions calculated in the present work at the different incident proton energies. The Rutherford scattering defines the general shape of the angular distribution at low energies. With the incident energy growth the interference between nuclear and Coulomb scattering shows up in the angular distributions.

The fission cross section calculated by GNASH code is shown in Fig.47 in comparison with the measured data [42,43], ALICE/ASH code calculations, the systematics values [23] and the data evaluated in Ref.[30]. The reasonable agreement is observed for all kind of the data. Fig.48 presents the relative contribution of different nuclei produced following the particle emission to the total (p,f) cross section. The fission of americium and plutonium isotopes provides the main proportion of the total fission cross section. As the incident energy growth the dominant role of americium isotopes drops down and is replaced by plutonium isotopes at the energy above 100 MeV.

The neutron and proton production cross sections calculated with GNASH code and ALICE/ASH code are compared in Fig.49. Figure 50 shows the relative contribution of different nuclei producing during the de-excitation process in the neutron production cross section presented in Fig.49. The yield of the prompt fission neutrons is not considered yet. The total neutron production cross section, which includes also the neutron emission from the fission fragments, is shown in Fig.51. The part of this cross section concerning the post-fission events only is presented in Fig.51 too.

Figure 52 illustrates the spectra of neutrons calculated in the present work using GNASH code, ALICE/ASH code and the CASCADE/INPE code [44]. The CASCADE/INPE code is based on the intranuclear cascade evaporation model. The agreement between the results obtained using different nuclear models and codes is better for the primary proton energy E_p=100 MeV, than for the energy E_p=250 MeV. In the present work GNASH code calculations were adopted as the most reliable ones and the corresponding spectra have been included in the evaluated data files.

The total proton production cross section together with the contribution from post-fission evaporation is presented in Fig.53. The relative contribution of the various nuclei in the total proton yields

is shown in Fig.54. At the energies up to 250 MeV the proton emission from excited nucleus with Z=95 plays the dominant role in the total proton yield.

Figures 55 and 56 show deuteron, triton, ^{3}He and α-production cross section together with the post-fission contributions calculated in the present work. The cross sections estimated with systematics at 62, 90 and 160 MeV are also shown in Figs.55 and 56.

Figure 57 presents the γ-production cross section for ^{239}Pu. One can see that the most contribution to this cross section is due to γ-emission followed by the fission.

$^{238}Pu, ^{240}Pu, ^{241}Pu, ^{242}Pu$

The experimental data are not available for the considered plutonium isotopes. The figures below show the major characteristics of the proton interactions with plutonium isotopes at the energies up to 250 MeV. Evaluated reaction cross sections are shown in Fig.58. Fission cross sections for 238Pu, 239Pu, 240Pu, 241Pu and 242Pu are compared in Fig.59. Neutron production cross sections including the neutron yield from (p,xnypzα) reactions and the pre-fission contribution are shown in Fig.60. Total neutron yield is presented in Fig.61. Total γ-production cross section is shown for various plutonium isotopes in Fig.62.

5. Conclusion

New data evaluation has been performed for ^{239}Pu, ^{239}Pu, ^{240}Pu, ^{241}Pu and ^{242}Pu in the intermediate energy region. For the first time the evaluated data for plutonium isotopes were obtained for neutron and proton induced reactions at the energies up to 250 MeV (see Table 8).

The evaluation procedure has included the application of the theoretical models and the analysis of the available experimental data. The coupled channel optical model, pre-compound and equilibrium models were used for nuclear reaction characteristics calculation. The neutron data obtained were combined with the JENDL-3.3 data at the energy of 20 MeV to get full data set at the energies from 10^{-5} eV to 250 MeV. The data for the proton induced reactions were evaluated in the energy region from 1 to 250 MeV.

Acknowledgements

Authors are grateful to Dr. S. Chiba, Research Group of Hadron Science, and members of Nuclear Data Center, for their valuable discussions. The author, A.Yu. Konobeyev, also thank Japan Atomic Energy Research Institute, for giving the opportunity to perform this work.

References

[1] M.Kawai, T.Yoshida, K.Hida JENDL-3.3 data file for ^{239}Pu, Evaluation: March 1987, last revision: 14 June 2001, private communication.

[2] T.Murata, T.Kawano, T.Nakagawa JENDL-3.3 data file for ^{240}Pu, Evaluation: February 2000, last revision: 4 August 2000, private communication.

[3] Y.Nakajima, T.Kawano, JENDL-3.3 data file for ^{241}Pu, Evaluation: February 2000, last revision: 31 March 2000, private communication.

[4] T.Murata,T.Kawano JENDL-3.3 data file for ^{242}Pu, Evaluation: March 2000, last revision: 18 May 2000, private communication.

[5] A.Yu.Konobeyev, T.Fukahori, O. Iwamoto, Neutron and Proton Data Evaluation for ^{235}U and ^{238}U at the Energies up to 250 MeV, to be published.

[6] J.Raynal, ECIS96 code, unpublished.

[7] P.G.Young, E.D.Arthur, M.B.Chadwick, Comprehensive Nuclear Model Calculations: Theory and Use of GNASH Code, Proc. Int. Atomic Energy Agency Workshop on Nuclear Reaction Data and Nuclear Reactors, April 15-May 17, 1996, v.1, p.227; Report LANL, LA-12343-MS (1992).

[8] A.V.Ignatyuk, Level Densities, In: Handbook for Calculations of Nuclear Reaction Data, IAEA-TECDOC-1034, p.65 (1998).

[9] A.V.Ignatyuk, K.K.Istekov, G.N.Smirenkin, *Yadernaja Fizika* **29,** 875 (1979).

[10] C.Kalbach, *Phys. Rev.* **C32,** 1157 (1985).

[11] M.B.Chadwick, P.G.Young. D.C.George, Y.Watanabe, *Phys. Rev.* **C50,** 996 (1994).

[12] M.Blann, H.Vonach, *Phys. Rev.* **C28,** 1475 (1983).

[13] M.Blann, *Phys. Rev. Lett.* **28,** 757 (1972).

[14] F.E.Bertrand, R.W.Peelle, *Phys. Rev.* **C8**, 1045 (1973).

[15] A.Yu.Konobeyev, Yu.A.Korovin, M.Vecchi, *Kerntechnik* **64,** 216 (1999).

[16] A.Yu.Konobeyev, Yu.A.Korovin, P.E.Pereslavtsev, Code "ALICE/ASH" for Calculation of Excitation Functions, Energy and Angular Distributions of Emitted Particles in Nuclear Reactions, Report INPE, Obninsk, February 1997

[17] A.I.Dityuk, A.Yu.Konobeyev, V.P.Lunev, Yu.N.Shubin, New Advanced Version of Computer Code ALICE-IPPE, Report IAEA INDC(CCP)-410 (1998).

[18] J.M.Peterson, A.Bratenahl, J.P.Stoering, *Phys. Rev.* **120**, 521 (1960).

[19] K.A.Nadolny, F.L.Green, P.Stoler, Report USNDC-9, 170, (1973).

[20] P.G.Young, In: Handbook for Calculations of Nuclear Reaction Data, IAEA-TECDOC-1034, p.131 (1998).

[21] V.S.Barashenkov Cross sections of Interactions of Particle and Nuclei with Nuclei, JINR, Dubna (1993); http://www.nea.fr/html/dbdata/bara.html.

[22] V.S.Barashenkov, A.Polanski, Electronic Guide for Nuclear Cross sections, JINR, Dubna (1995).

[23] T.Fukahori, S.Pearlstein, Report BNL-45200 (1991).

[24] A.Yu.Konobeyev, Yu.A.Korovin, V.V.Lunev, P.E.Pereslavtsev A.Yu.Stan-kovsky, Evaluated Neutron Data File for ^{239}Pu up to 50 MeV, INPE, November 1995, revised: 15 May 1998.

[25] Yu.A.Korovin, A.Yu.Konobeyev, P.E.Pereslavtsev, A.Yu.Stankovsky, Proc. Int. Conf. for Nuclear Science and Technology, Trieste, May 19-24, p. 851 (1997).

[26] G.W.Carlson, J.W.Behrens, *Nucl. Sci. Eng.* **66**, 205 (1978).

[27] P.W.Lisowski, J.L.Ullmann, S.J.Balestrini, A.D.Carlson, O.A.Wasson, N.W.Hill, Proc. Int. Conf. for Nuclear Data for Science and Technology, Mito, May 30- June 3, p97 (1988).

[28] P.Staples, K.Morley, *Nucl. Sci. Eng.* **129**, 149 (1998).

[29] O.Shcherbakov, ISTC No.609 (2000).

[30] S.Yavshits, O.Grudzevich, G.Boykov, V.Ippolitov, Proc. of the 2000 Symposium on Nuclear Data, Nov. 16-17, 2000, Tokai, Japan, JAERI-Conf 2001-006, INDC(JPN)-188/U, p.277 (2001).

[31] J.Frehaut, EXFOR 21685 (1980).

[32] A.Yu.Konobeyev, Yu.A.Korovin, *Atomic Energy* **85** (1998) 556 (translated from Russian Journal "*Atomnaja Energija*").

[33] R.F.Coleman, B.E.Hawker, L.P.O'connor, J.L.Perkin, *Proceedings of the Physical Society (London)* **73**, 215 (1959).

[34] A.Yu.Konobeyev, V.P.Lunev, Yu.N.Shubin, *Nuovo Cimento* **111A**, 445 (1998).

[35] A.Yu.Konobeyev, V.P.Lunev, Yu.N.Shubin, *Nucl. Instr. Meth. Phys. Res.* **B108**, 233 (1996).

[36] J.W.Behrens, R.S.Newbury, J.W.Magana, *Nucl. Sci. Eng.* **66**, 433 (1978).

[37] M.S.Moore, P.W.Lisowski, G.L.Morgan, G.F.Auchampaugh, R.E.Shamu, Proc. Int. Conf. on Nuclear Cross sections for Technology, Knoxville, Tennessee, Oct 22 – 26, 1979, p.703.

[38] J.W.Behrens, G.W.Carlson, *Nucl. Sci. Eng.* **68**, 128 (1978).

[39] V.S.Barashenkov, V.D.Toneev, Interaction of High Energy Particles and Nuclei with Nuclei (Atomizdat, Moscow, 1972), [English translation: FTD-ID(RS)T-1069-77, Wright-Patterson Air Force Base, Foreign Technology Division, Dayton, Ohio (1977)].

[40] T.W.Burrows, D.Dempsey, The Bibliography of Integral Charged Particle Nuclear Data, BNL-NCS-50640 (1980).

[41] A.V.Prokofiev, *Nucl. Instr. Meth. Phys. Res.* **A463**, 557 (2001).

[42] T.Ohtsuki, Y.Nagame, K.Tsukada, N.Shinohara et al., *Phys. Rev.* **C44**, 1405 (1991).

[43] A.N.Smirnov, I.Yu.Gorshkov, A.V.Prokofiev, V.P.Eismont, Proc. 21st Intern. Symp. on Nuclear Phys., Gaussig, Germany, November 4-8, 1991, p.214; V.P.Eismont, A.V.Prokofiev, A.N.Smirnov, Proc. Int. Conf. for Nuclear Science and Technology, Gatlinburg, May 9-13, 1994, p.397.

[44] V.S.Barashenkov, A.Yu.Konobeyev, Yu.A.Korovin, V.N.Sosnin, *Atomnaja Energija* **87**, 283 (1999).

Table 1. The relative contribution (%) of the isotopes with Z=94 in the total fission cross sections for neutron interactions with plutonium isotopes.

Energy of neutrons (MeV)	^{239}Pu	^{240}Pu	^{241}Pu	^{242}Pu
50	90.36	91.64	92.91	93.86
100	63.26	65.31	67.52	69.94
150	46.62	48.43	49.81	52.23
250	31.20	31.64	32.45	34.59

Table 2. The relative contribution (%) of the isotopes with Z=93 in the total fission cross sections for neutron interactions with plutonium isotopes.

Energy of neutrons (MeV)	^{239}Pu	^{240}Pu	^{241}Pu	^{242}Pu
50	9.218	8.070	6.824	5.949
100	32.54	30.87	28.58	26.89
150	45.24	43.63	42.09	40.33
250	50.27	50.80	50.22	49.11

Table 3. The relative contribution (%) of the isotopes with Z=92 in the total fission cross sections for neutron interactions with plutonium isotopes.

Energy of neutrons (MeV)	^{239}Pu	^{240}Pu	^{241}Pu	^{242}Pu
50	0.4242	0.2875	0.2697	0.1897
100	4.019	3.702	3.806	3.115
150	6.580	6.675	6.941	6.542
250	9.049	9.087	9.323	9.381

Table 4. The cross sections for (n,p), (n,d), (n,α) reactions at the energy 14.5 MeV and for (n,t) reaction at 14.6 MeV predicted by semi-empirical systematics [32,34,35] in millibarns for various plutonium isotopes. (The cross section for (n,d) reaction does not contain the contribution from (n,np) reaction)

Mass number	(n,p)	(n,d)	(n,t)	(n,α)
236	2.36	0.306	0.0381	0.627
237	1.94	0.243	0.0598	0.474
238	1.57	0.189	0.0319	0.348
239	1.26	0.144	0.0508	0.248
240	0.987	0.107	0.0265	0.169
241	0.761	0.0768	0.0428	0.110
242	0.573	0.0533	0.0218	0.0661
243	0.421	0.0353	0.0358	0.0362
244	0.298	0.0220	0.0177	0.0172

Table 5. Deuteron, triton, ^{3}He and α-production cross sections obtained according to the systematics from Ref.[5] at the primary proton energy 62 MeV in millibarns for various plutonium isotopes.

Mass number	(p,d)x	(p,t)x	(p,^{3}He)x	(p,α)x
236	91.68	23.94	2.29	39.19
237	91.89	24.23	2.22	38.21
238	92.10	24.52	2.15	37.25
239	92.30	24.81	2.09	36.33
240	92.51	25.09	2.02	35.44
241	92.71	25.37	1.96	34.58
242	92.91	25.65	1.91	33.74
243	93.10	25.93	1.85	32.94
244	93.30	26.20	1.80	32.15

Table 6. Deuteron, triton, ^{3}He and α-production cross sections obtained according to the systematics from Ref.[5] at the primary proton energy 90 MeV in millibarns for various plutonium isotopes.

Mass number	(p,d)x	(p,t)x	(p,^{3}He)x	(p,α)x
236	157.86	43.50	8.79	89.70
237	158.83	44.13	8.73	88.22
238	159.80	44.74	8.68	86.77
239	160.76	45.36	8.63	85.36
240	161.71	45.97	8.57	83.99
241	162.65	46.57	8.52	82.65
242	163.59	47.17	8.47	81.34
243	164.52	47.76	8.42	80.06
244	165.44	48.35	8.37	78.81

Table 7. Deuteron, triton, ^{3}He and α-production cross sections obtained according to the systematics from Ref.[5] at the primary proton energy 160 MeV in millibarns for various plutonium isotopes.

Mass number	(p,d)x	(p,t)x	(p,^{3}He)x	(p,α)x
236	119.35*	33.13	11.13	95.60
237	120.25	33.61	11.08	95.11
238	121.13	34.09	11.04	94.62
239	122.01	34.56	10.99	94.13
240	122.88	35.03	10.94	93.65
241	123.74	35.50	10.90	93.17
242	124.60	35.96	10.85	92.70
243	125.45	36.42	10.81	92.22
244	126.29	36.87	10.76	91.76

* There is the probable contradiction between deuteron and triton production cross sections at 90 MeV (Table 6) and at 160 MeV. It should be noted that the systematics values reflect only the state of the available measured data.

Table 8. Status of intermediate energy nuclear data evaluation for plutonium isotopes.

Organization	Year	Primary particle	Maximal primary energy	Basic data below 20 MeV for neutron data file	Reference
^{239}Pu					
INPE, FZK	1995	neutrons	50 MeV	JENDL-3.2	[24,25]
JAERI	2001	neutrons, protons	250 MeV	JENDL-3.3	This work
^{240}Pu					
INPE, FZK	1997	neutrons	50 MeV	ENDF/B-VI	[25]
JAERI	2001	neutrons, protons	250 MeV	JENDL-3.3	This work
^{238}Pu, ^{241}Pu, ^{242}Pu					
JAERI	2001	neutrons, protons	250 MeV	JENDL-3.3	This work

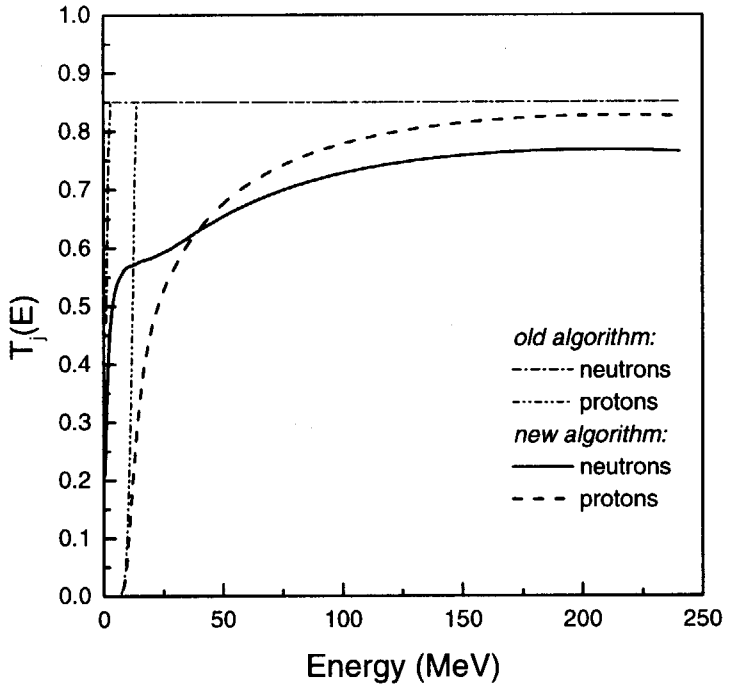

Fig.1 Emission probability of nucleons calculated as described in Ref.[7] ("old algorithm") and with the help of Eqs.(2)-(4) ("new algorithm").

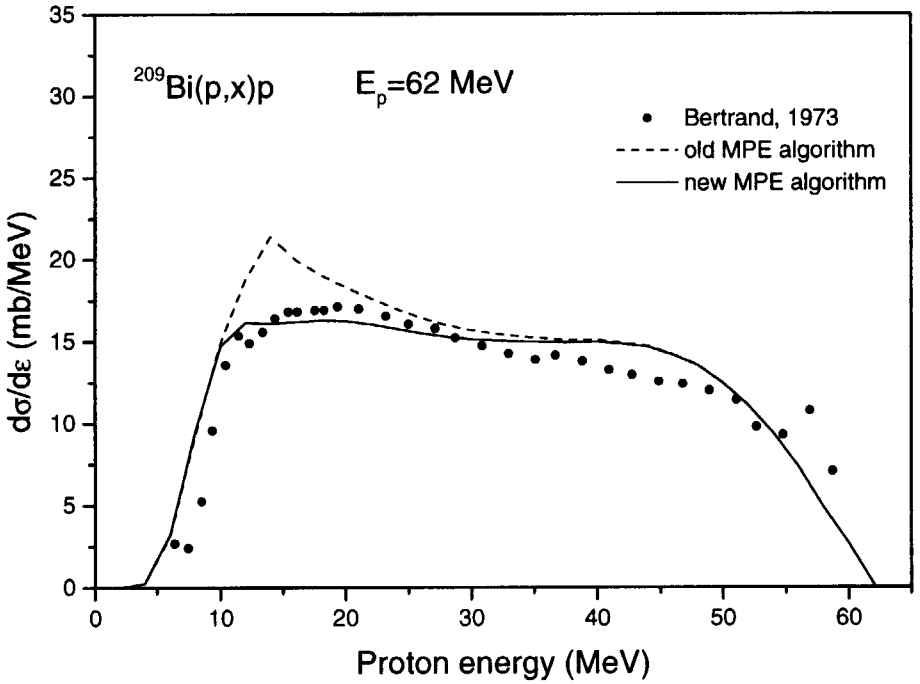

Fig.2 Energy distribution of secondary protons in p+^{209}Bi interactions at the energy E_p=62 MeV calculated using new algorithm of multi-particle emission from pre-compound states (MPE, solid line) and old one (dashed line) for $T_j(E)$ calculation. The experimental data are from Ref.[14].

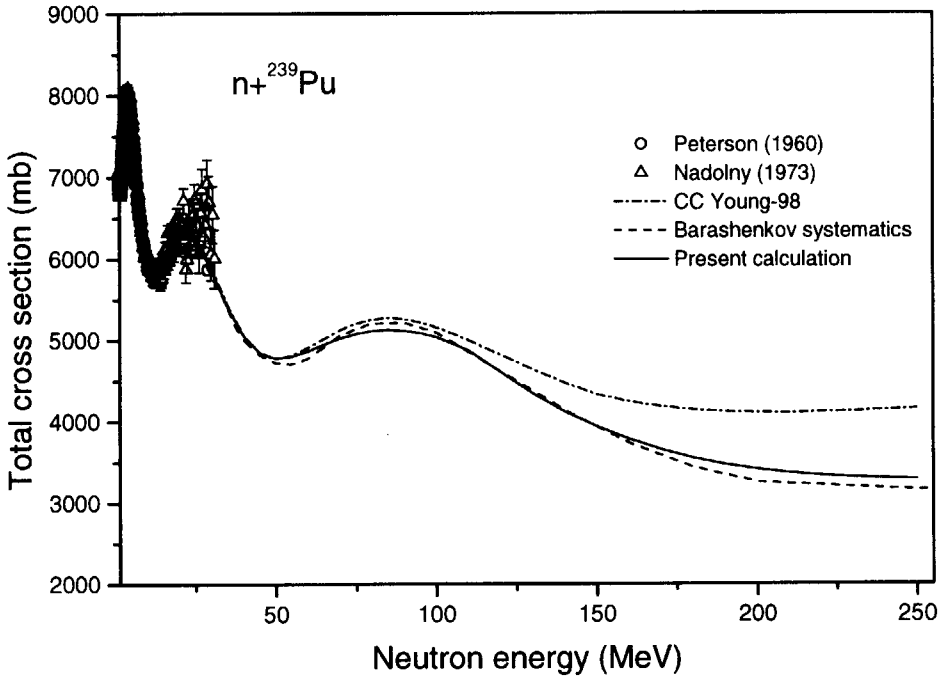

Fig.3 Total neutron cross section for ^{239}Pu obtained using different sets of the coupled channel optical model parameters and estimated according to the systematics [21,22]. The measured data are taken from Refs.[18,19].

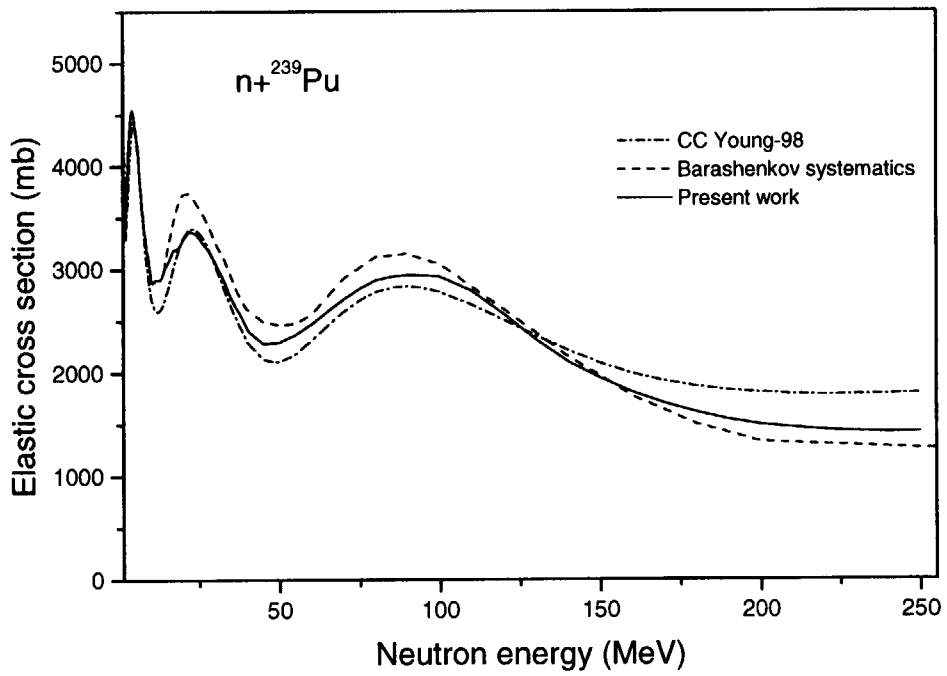

Fig.4 Elastic cross sections for ^{239}Pu obtained in the present work, calculated by the coupled channel optical model with the parameters from Ref.[20] and estimated according to the systematics [21,22].

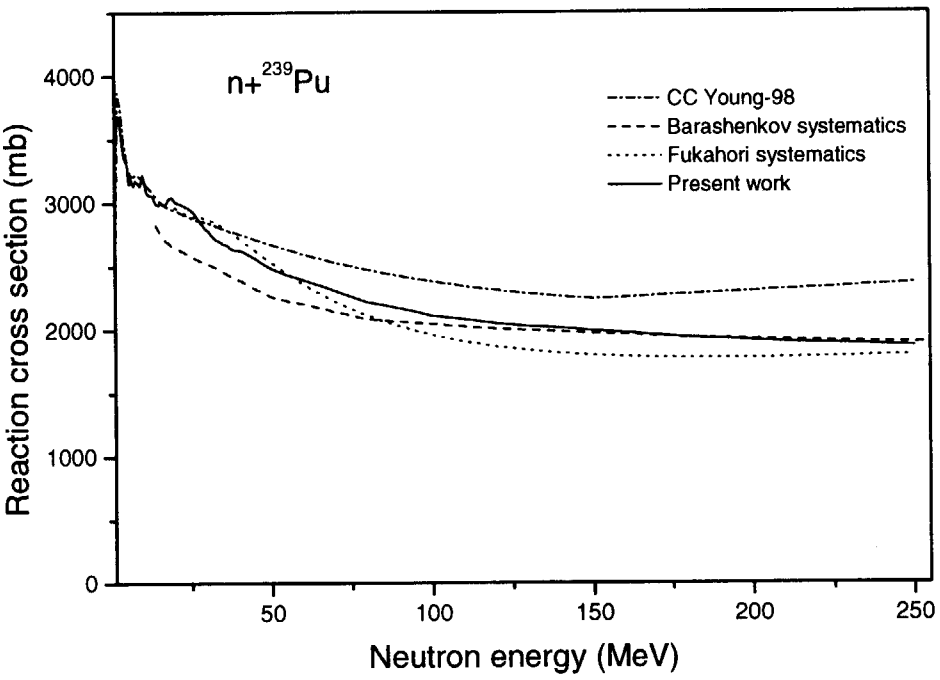

Fig.5 Reaction cross sections for ^{239}Pu obtained in the present work, calculated by the coupled channel optical model with the parameters from Ref.[20] and estimated according to the systematics [21,22] and [23].

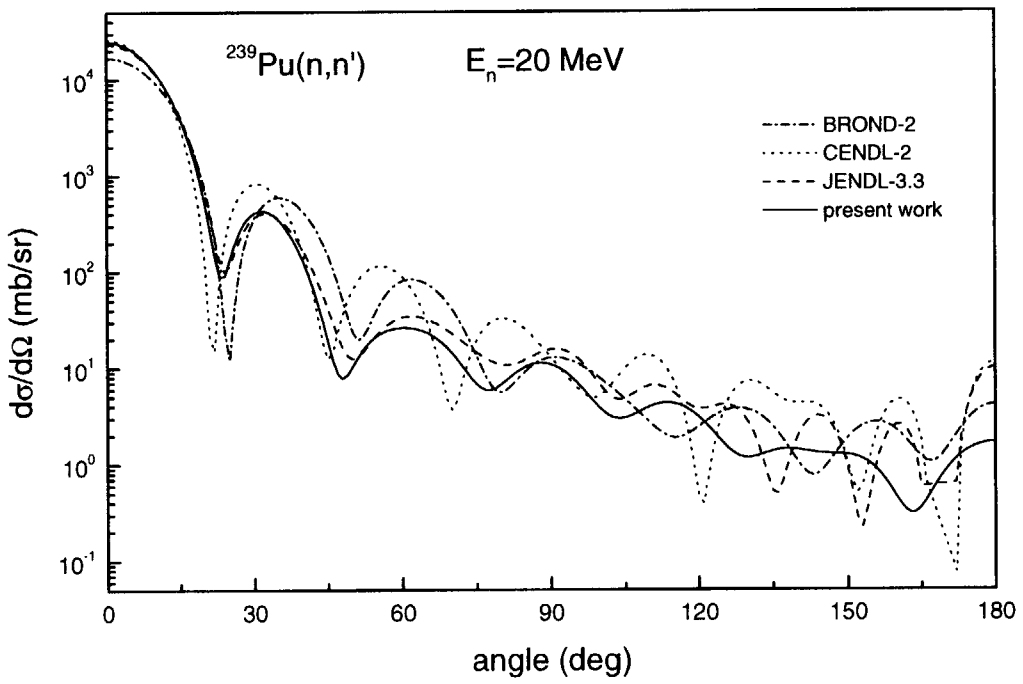

Fig.6 Elastic scattering angular distribution at the primary neutron energy E_n = 20 MeV obtained in the present work and taken from different data libraries. See comments in the text.

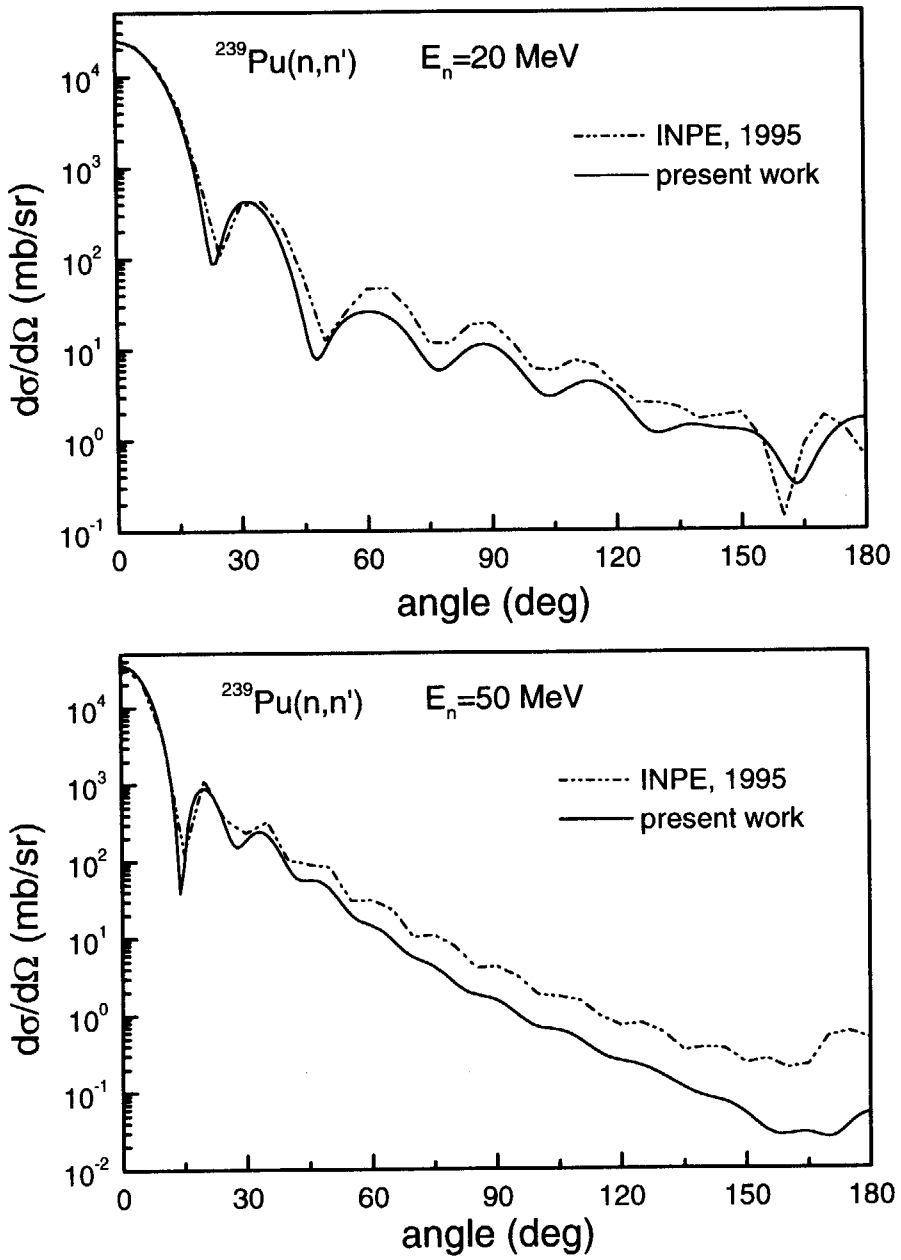

Fig.7 Elastic angular distribution for ^{239}Pu at the different neutron incident energy calculated in the present work (solid line) and evaluated in Refs.[24,25] (dashed-dotted line).

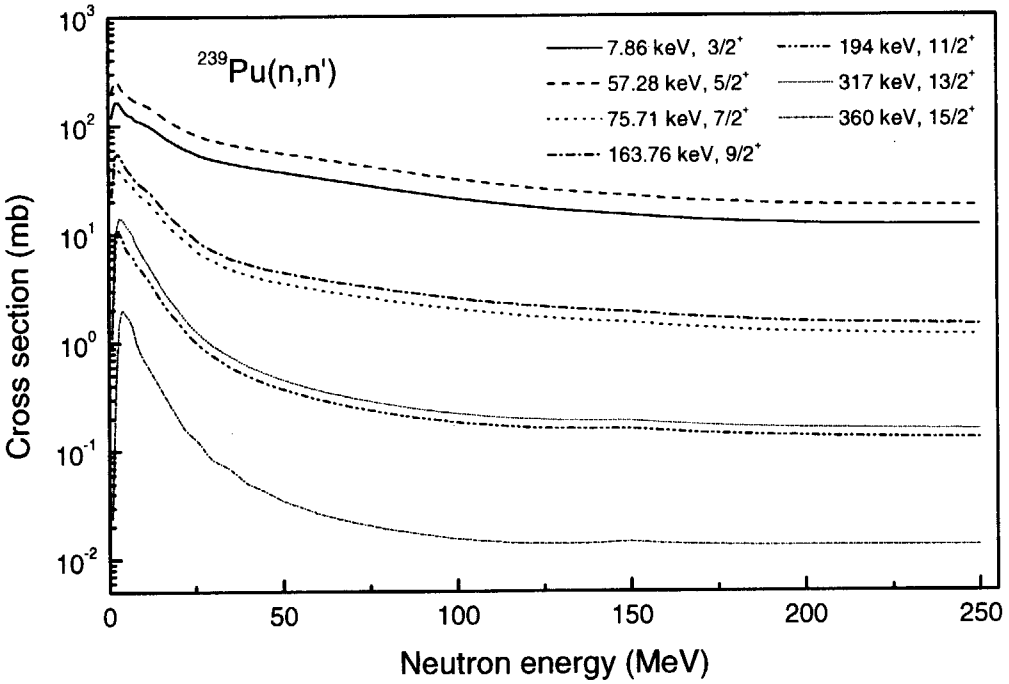

Fig.8 Direct neutron inelastic scattering cross sections calculated for ^{239}Pu for the excited levels $3/2^+$, $5/2^+$, $7/2^+$, $9/2^+$, $11/2^+$ and $15/2^+$ members of the ground-state rotational band.

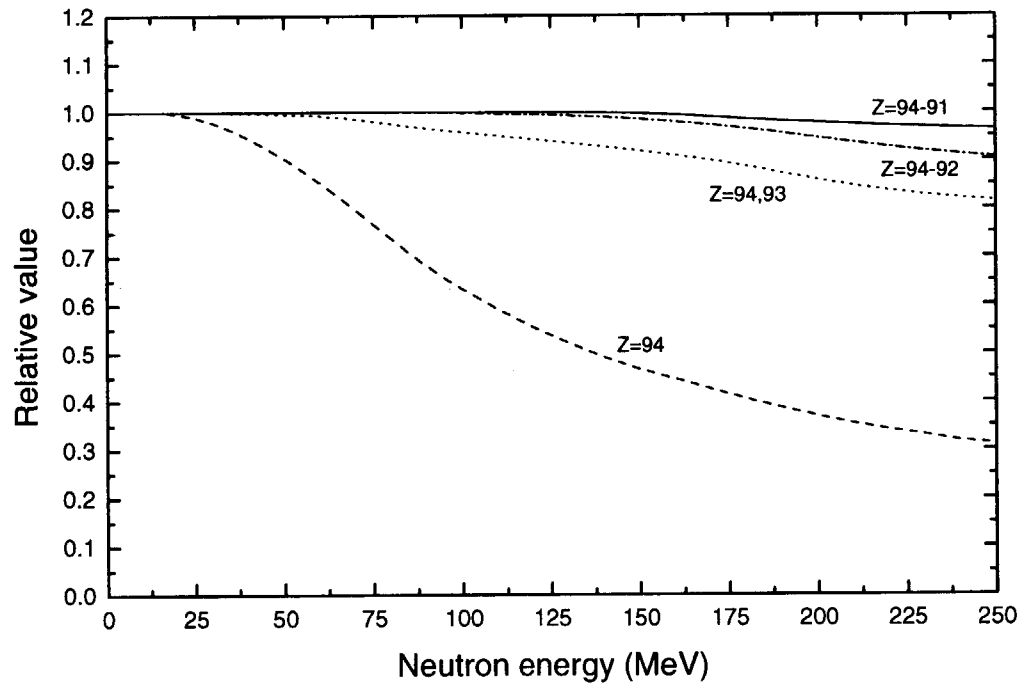

Fig.9 The relative contribution of the nuclei with the different atomic number in the total fission cross section for ^{239}Pu calculated by GNASH code.

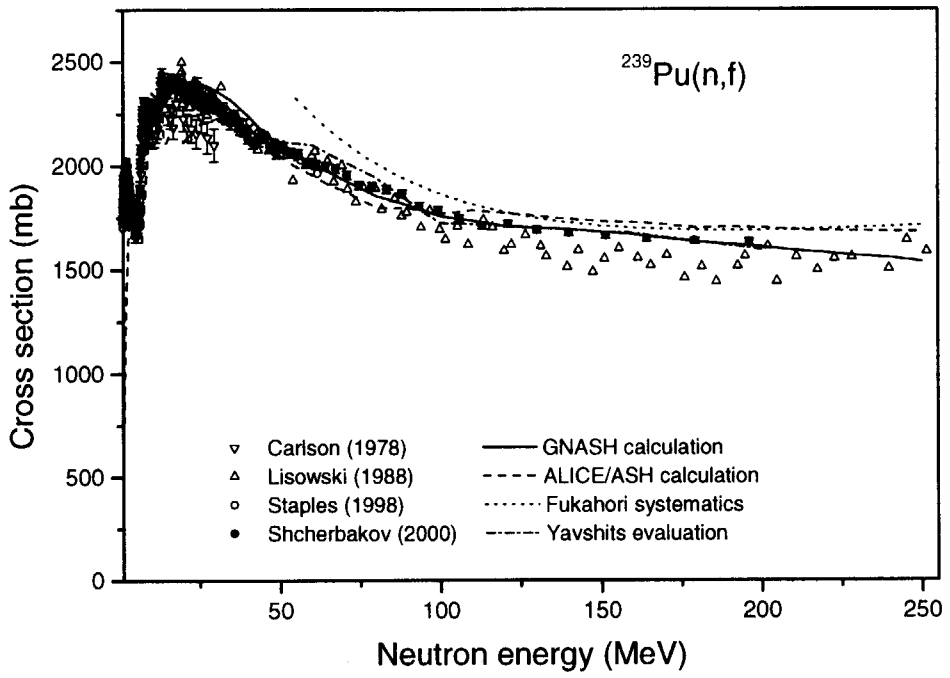

Fig.10 Fission cross section for ^{239}Pu calculated with GNASH and ALICE/ASH codes, cross section estimated using the systematics [23], data evaluated in Ref.[30] and measured in Refs.[26-29].

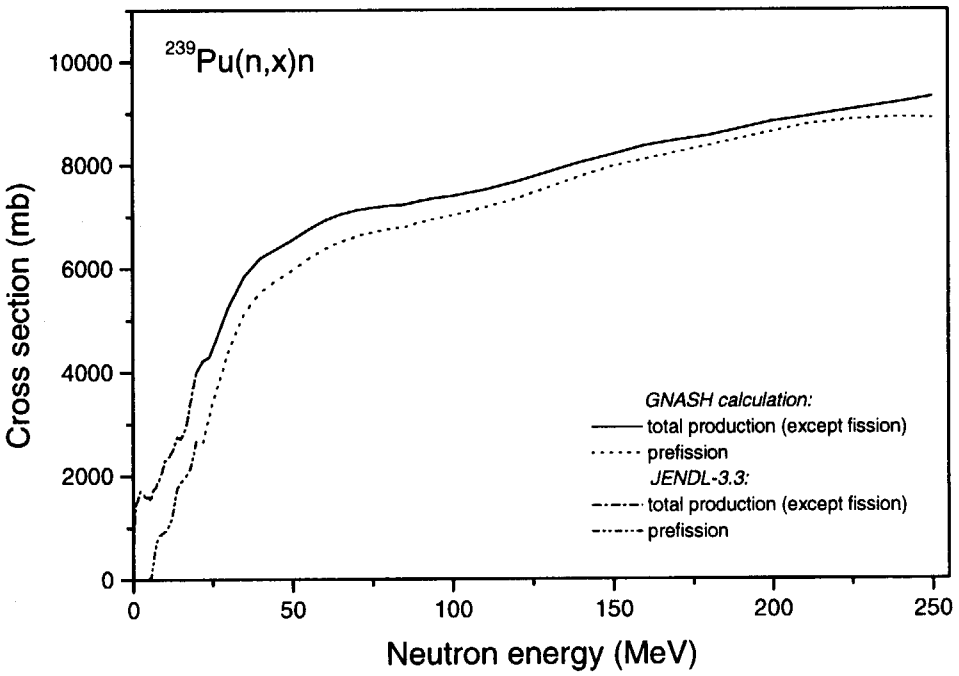

Fig.11 Neutron production cross section without the contribution from the post-fission evaporation for ^{239}Pu calculated by GNASH code and taken from JENDL-3.3 file.

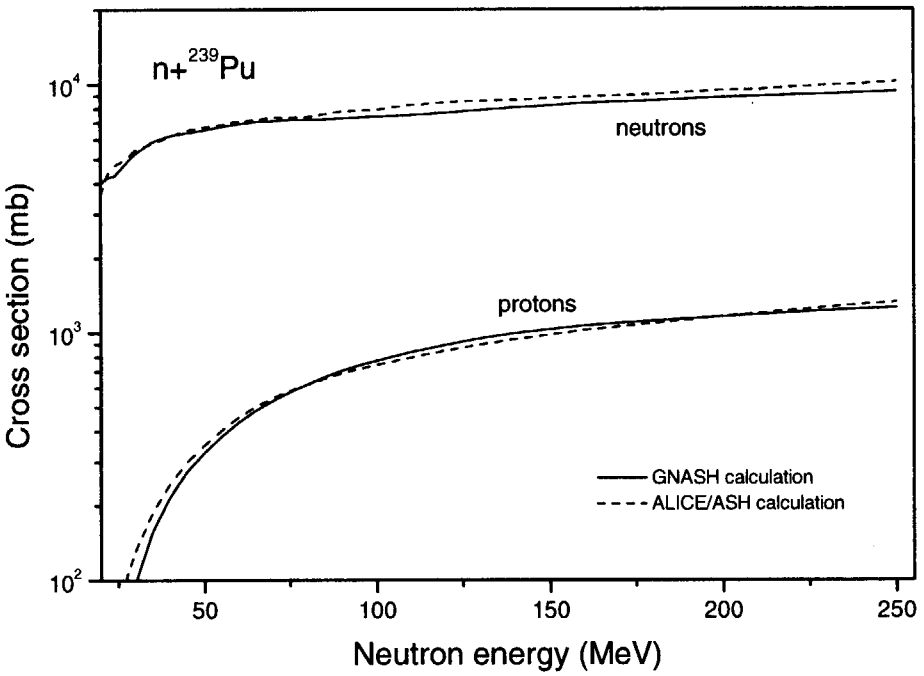

Fig.12 Comparison of the neutron and proton production cross sections calculated with GNASH code and ALICE/ASH code for ^{239}Pu without the contribution from the post-fission evaporation.

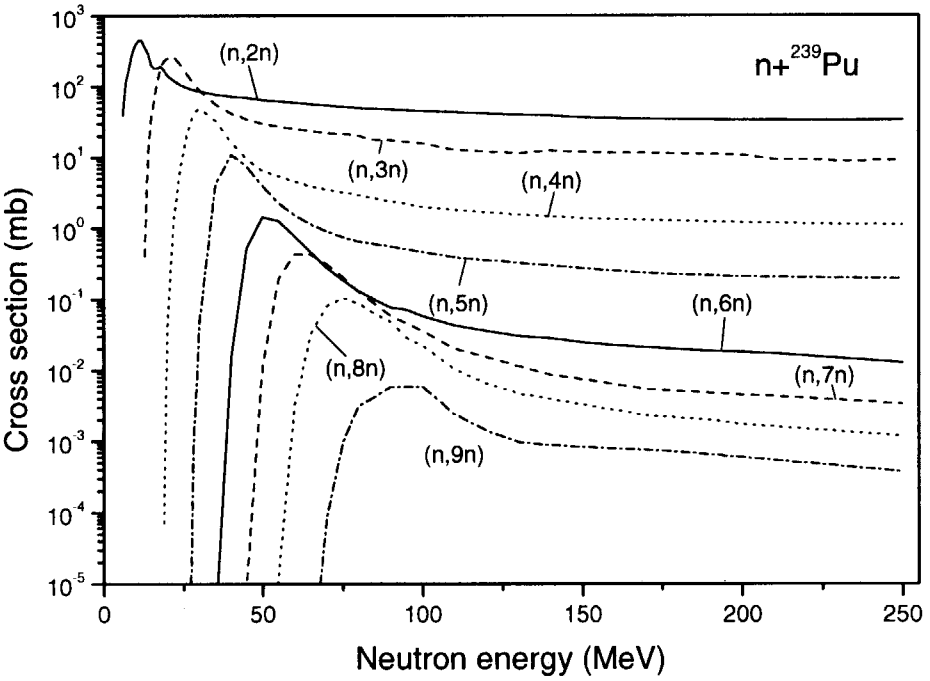

Fig.13 Evaluated (n,xn) reaction cross sections for ^{239}Pu.

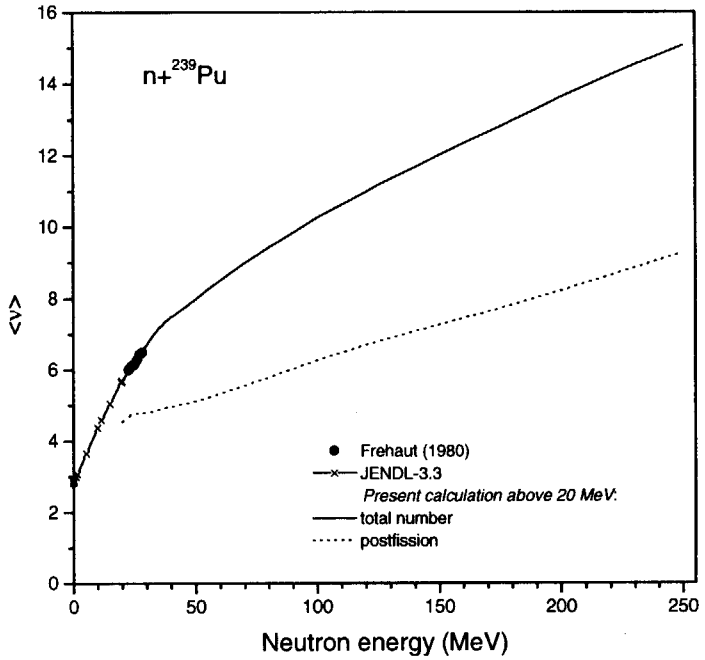

Fig.14 Total number of prompt fission neutrons (solid line) and neutrons emitted from the excited fission fragments (dotted line) evaluated in the present work for ^{239}Pu. Experimental data are from Ref.[31]. Below 20 MeV JENDL-3.3 data (—x—) are shown.

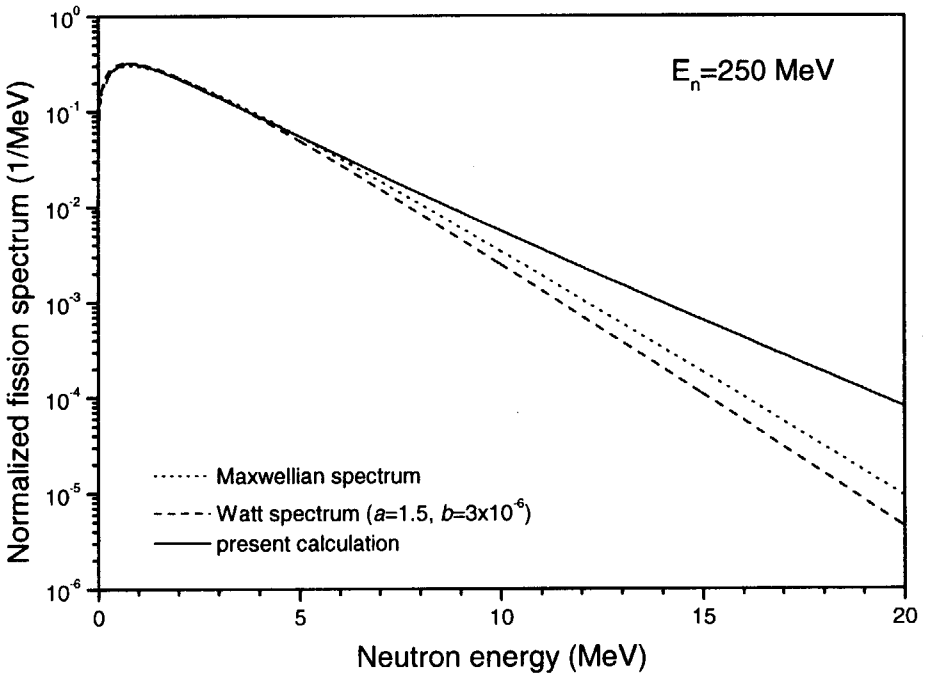

Fig.15 Normalized fission neutron spectrum for ^{239}Pu calculated in the present work (solid line), Watt spectrum (dashed line) and Maxwellian one (dotted line) for the primary neutron energy equal to 250 MeV. See comments in the text.

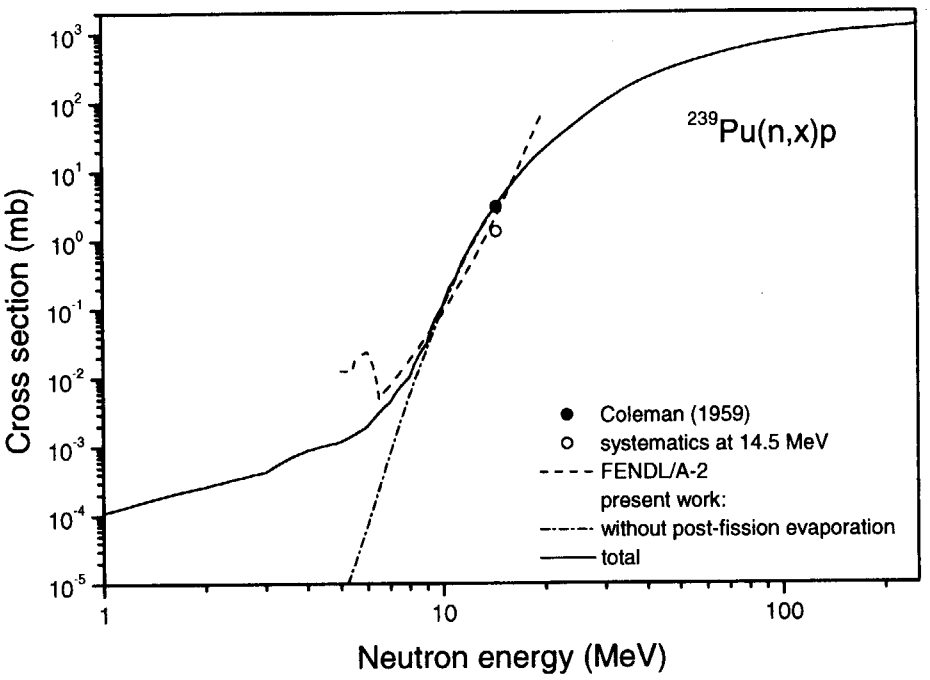

Fig.16 Total proton production cross section for ^{239}Pu, evaluated in the present work, obtained by the systematics [32], measured in Ref.[33] and taken from FENDL/A-2.

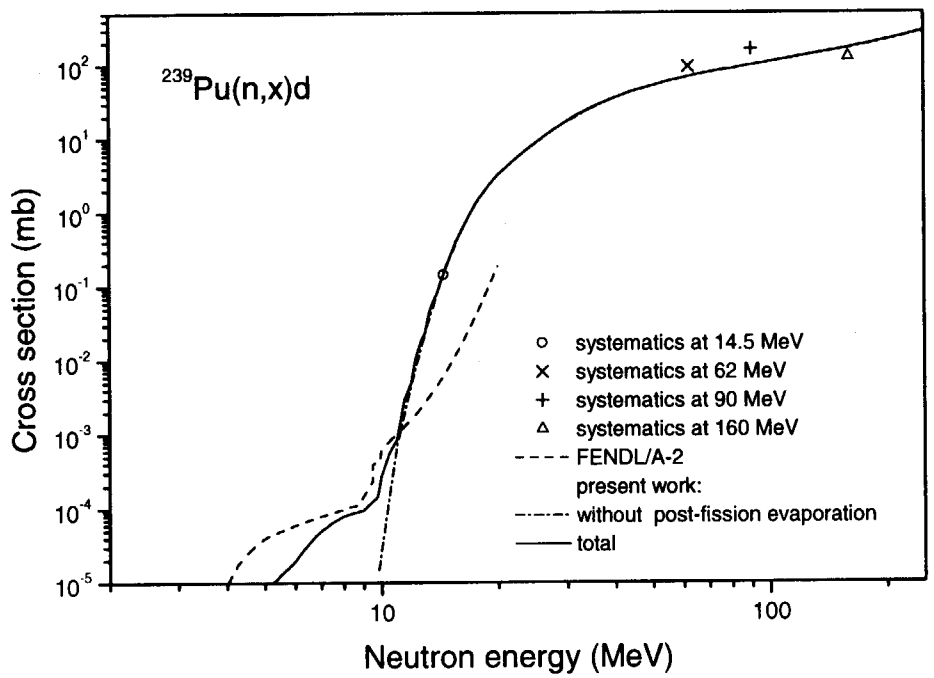

Fig.17 Total deuteron production cross section for ^{239}Pu, evaluated in the present work, obtained by the systematics [5,32] and taken from FENDL/A-2.

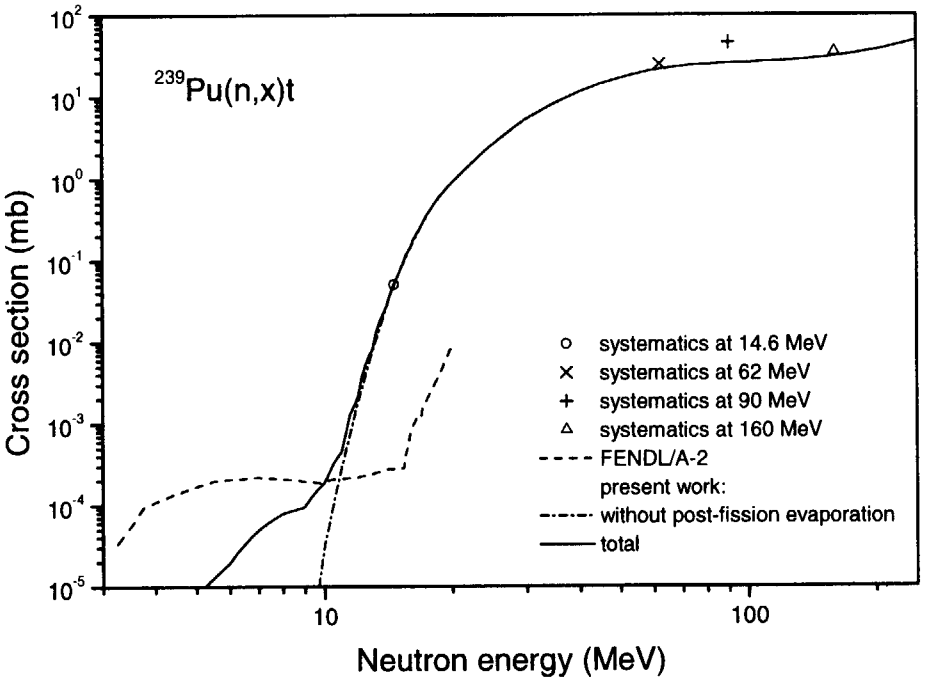

Fig.18 Total triton production cross section for ^{239}Pu, evaluated in the present work, obtained by the systematics [5,32,34] and taken from FENDL/A-2.

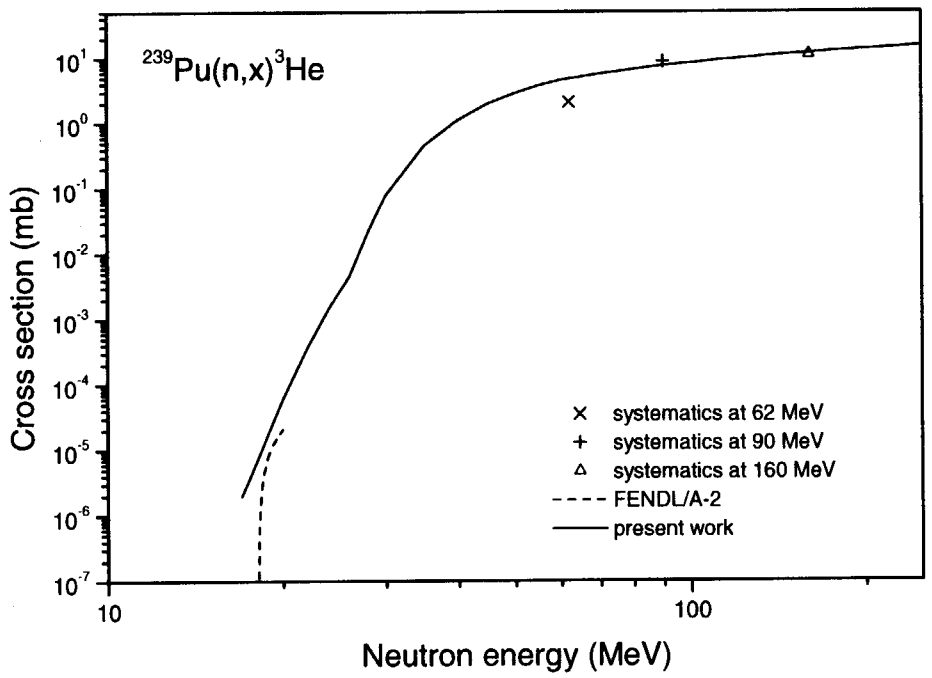

Fig.19 Total ^{3}He-production cross section for ^{239}Pu, evaluated in the present work, obtained by the systematics [5] and taken from FENDL/A-2.

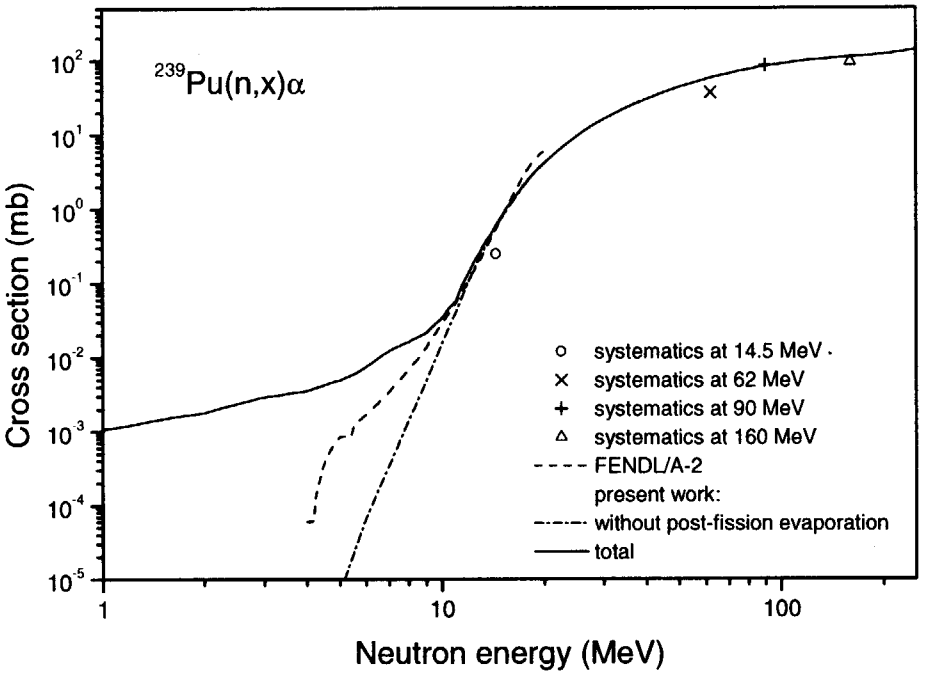

Fig.20 Total α-production cross section for ^{239}Pu, evaluated in the present work, obtained by the systematics [5,32,35] and taken from FENDL/A-2.

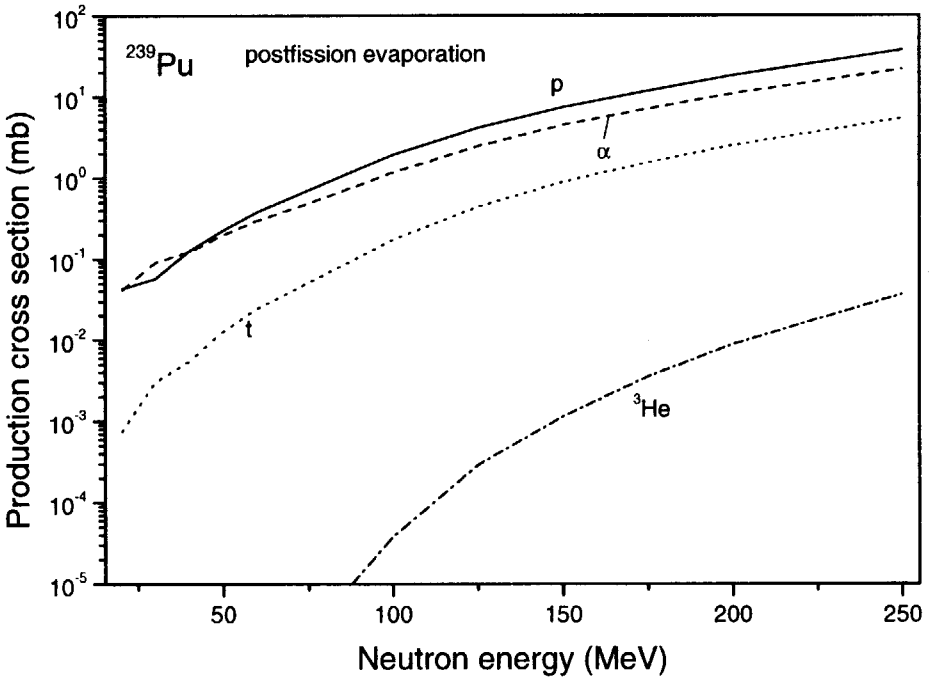

Fig.21 Calculated production cross section for protons, tritons, ^{3}He- and α-particles emitted from the excited fission fragments in n+^{239}Pu interactions.

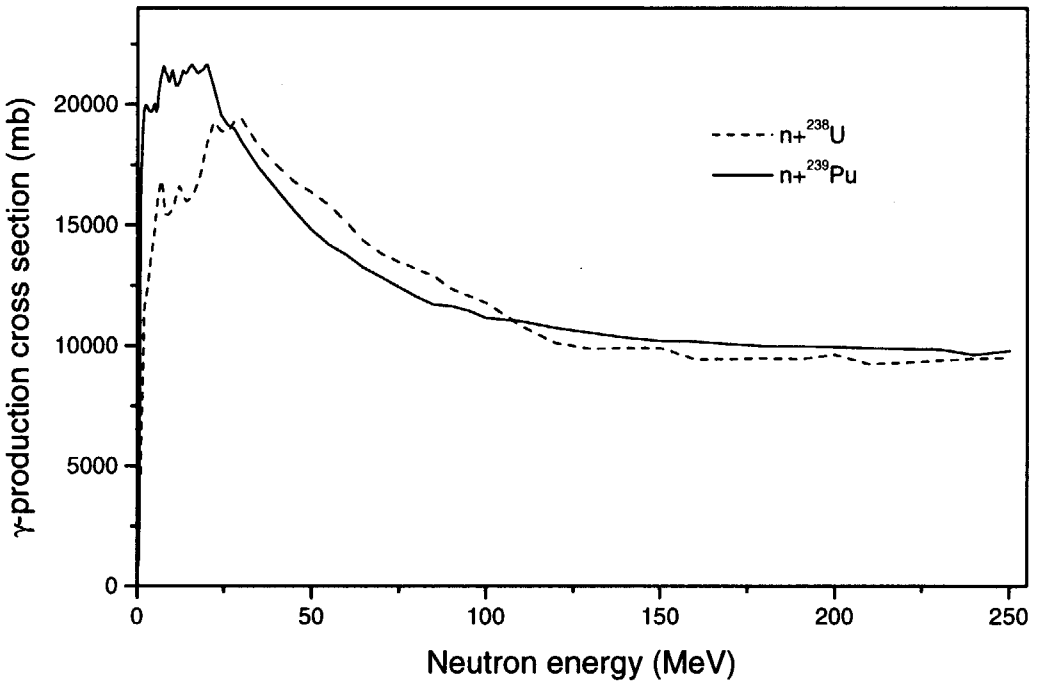

Fig.22 Total γ-production cross section for n+^{239}Pu interaction in the comparison with the data for ^{238}U.

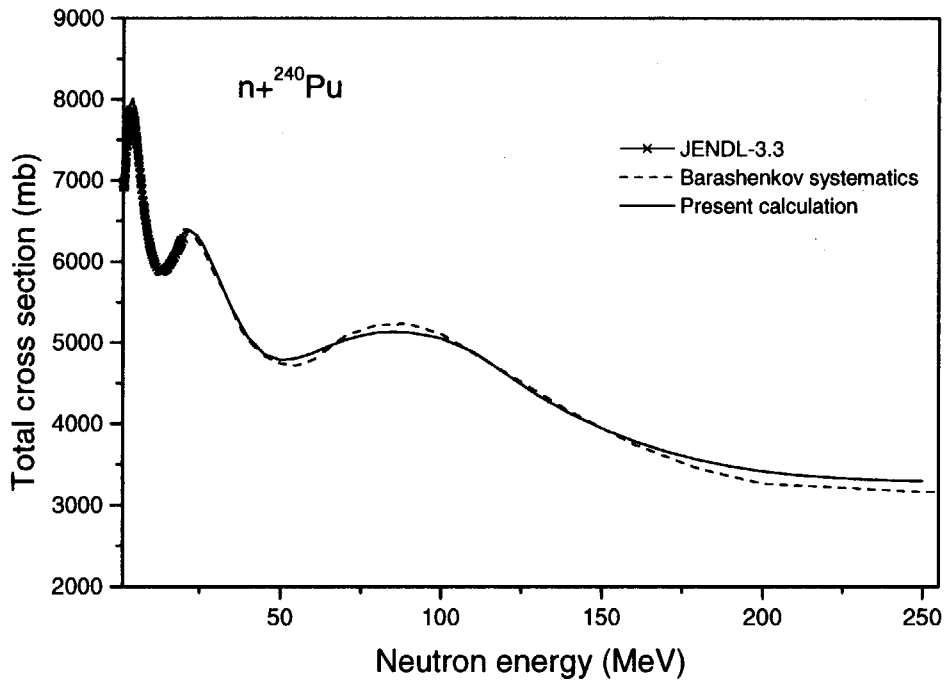

Fig.23 Total neutron cross section for ^{240}Pu calculated in the present work with coupled channel optical model, estimated by the systematics [21,22] and taken from JENDL-3.3.

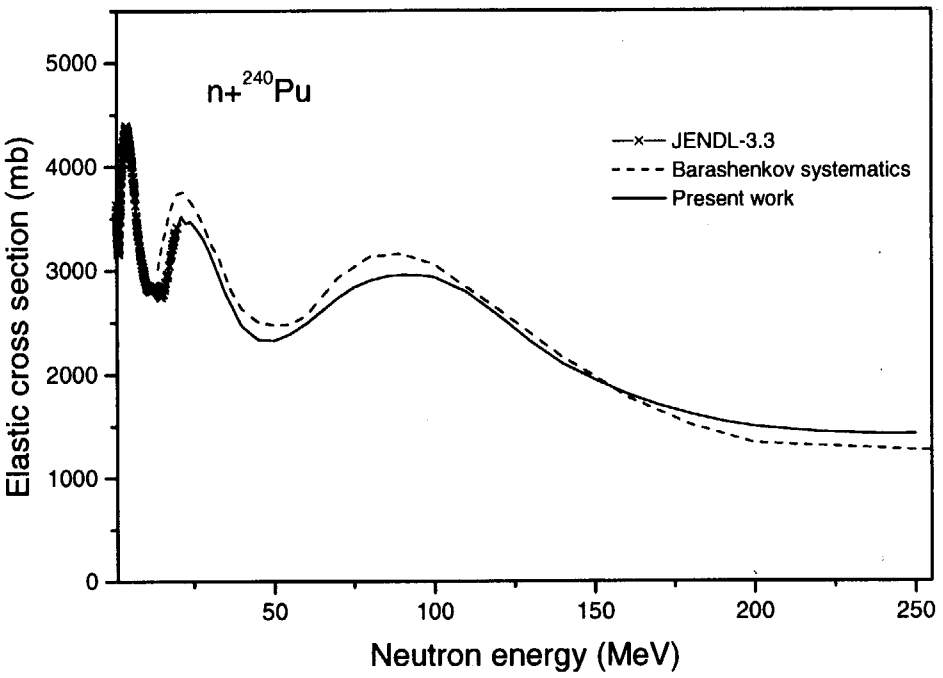

Fig.24 Elastic neutron cross section for ^{240}Pu obtained in the present work, estimated by the systematics [21,22] and taken from JENDL-3.3.

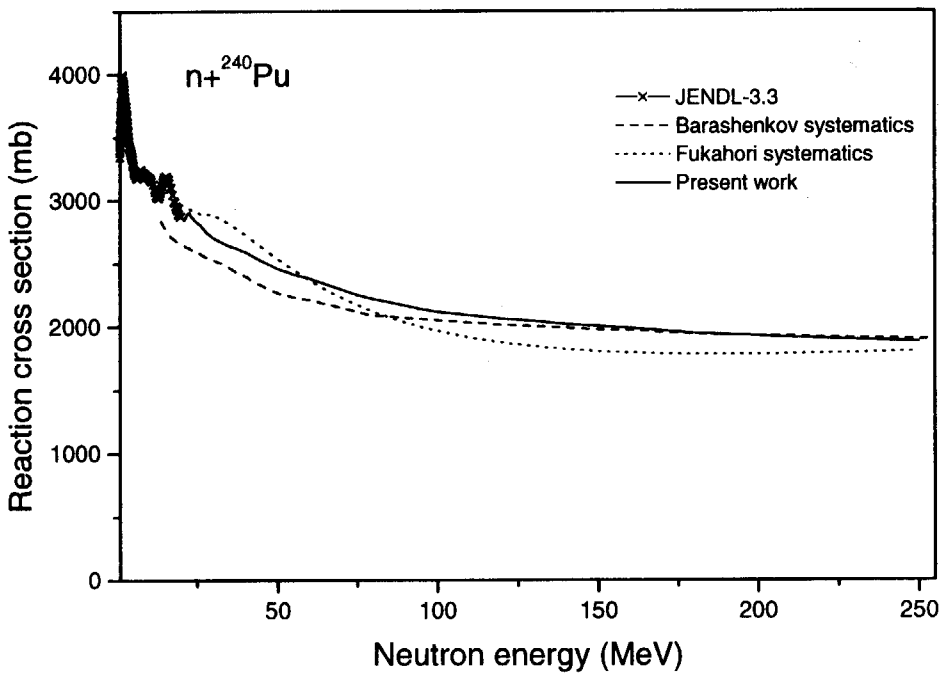

Fig.25 Reaction neutron cross section for ^{240}Pu obtained in the present work, estimated by the systematics [21-23] and taken from JENDL-3.3.

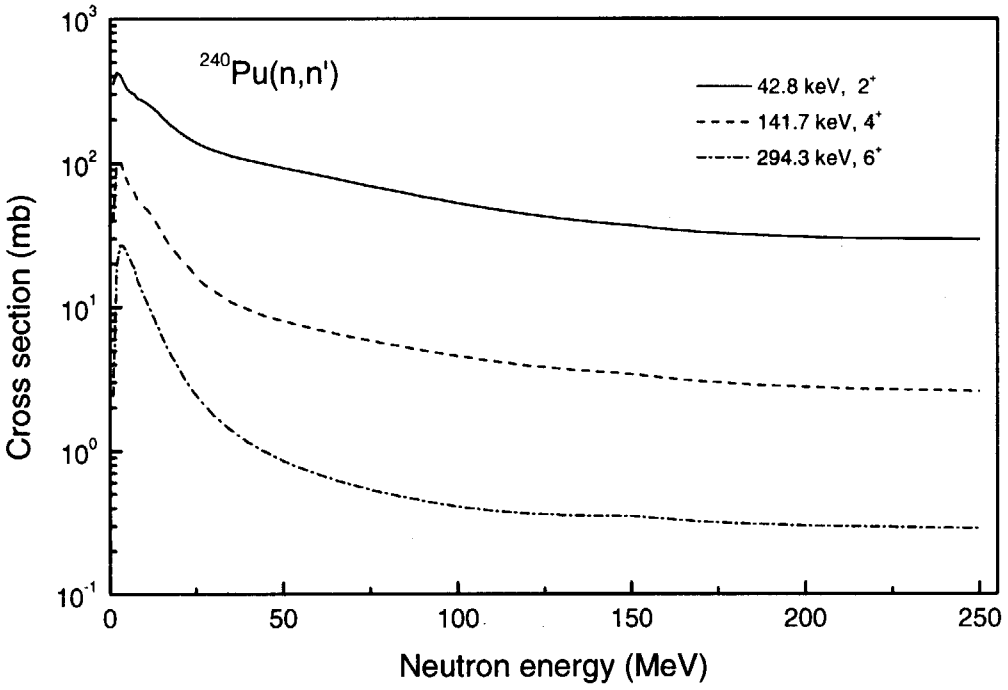

Fig.26 Direct neutron inelastic scattering cross sections calculated for ^{240}Pu for the lowest excited levels 2^+, 4^+ and 6^+.

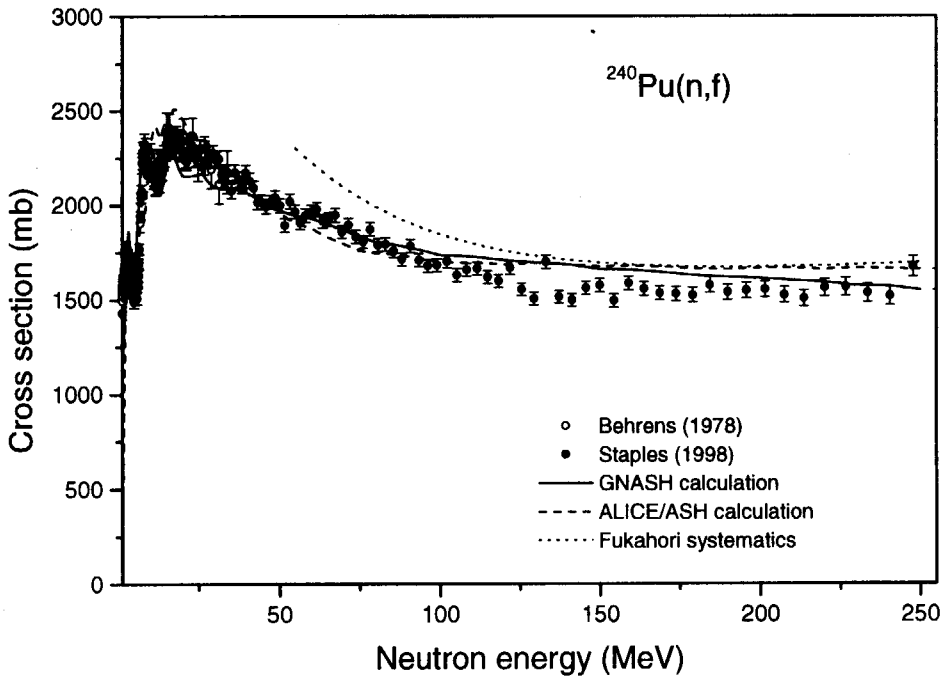

Fig.27 Fission cross section for ^{240}Pu calculated with GNASH code and ALICE/ASH code, cross section estimated using the systematics [23], data evaluated in Ref.[30] and measured in Refs.[28,36].

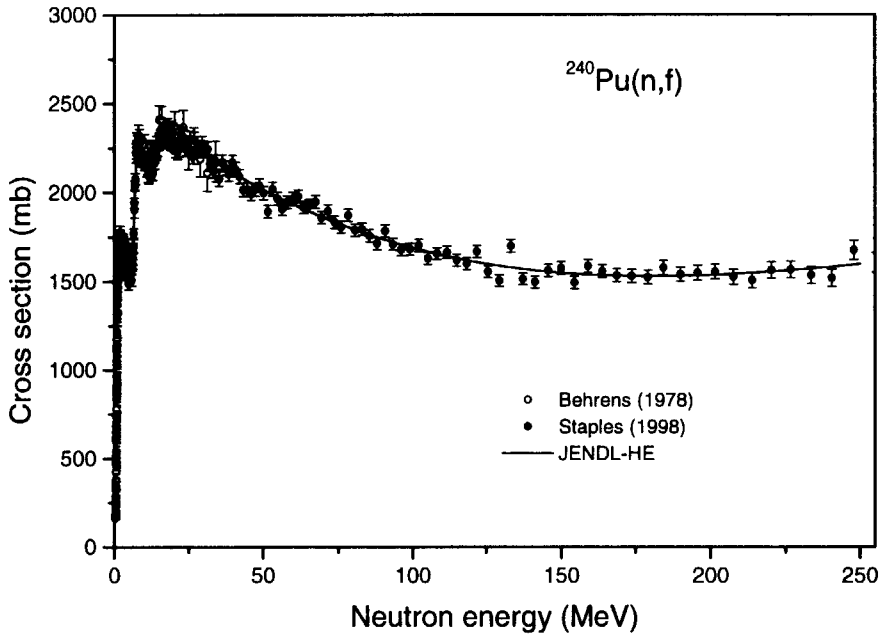

Fig.28 Recommended fission cross section for ^{240}Pu (solid line) and the experimental data from Refs.[28,36].

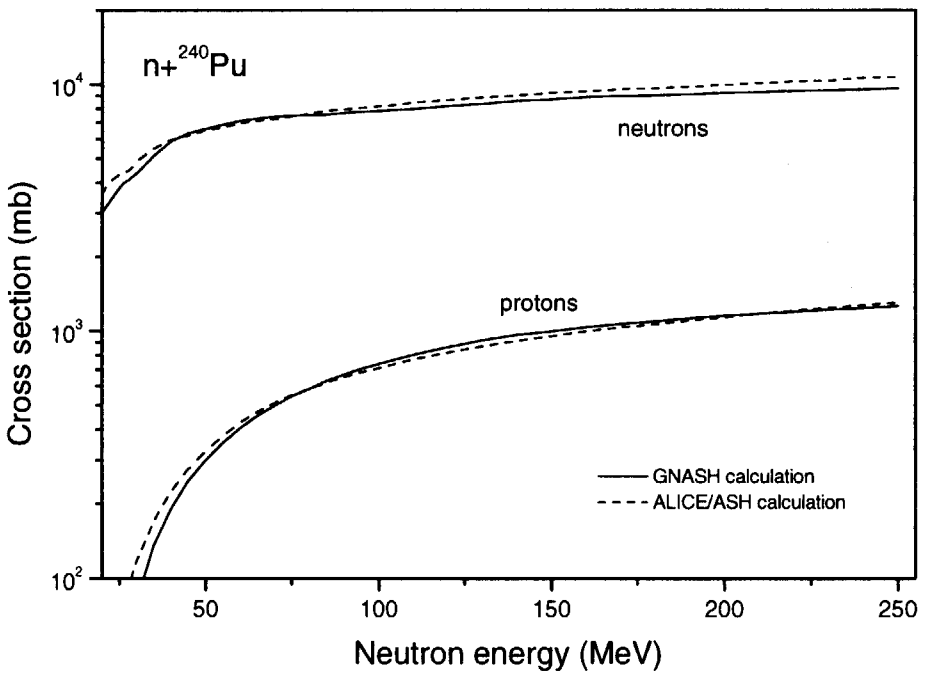

Fig.29 Comparison of the neutron and proton production cross sections calculated with GNASH code and ALICE/ASH code for ^{240}Pu without the contribution from the post-fission evaporation.

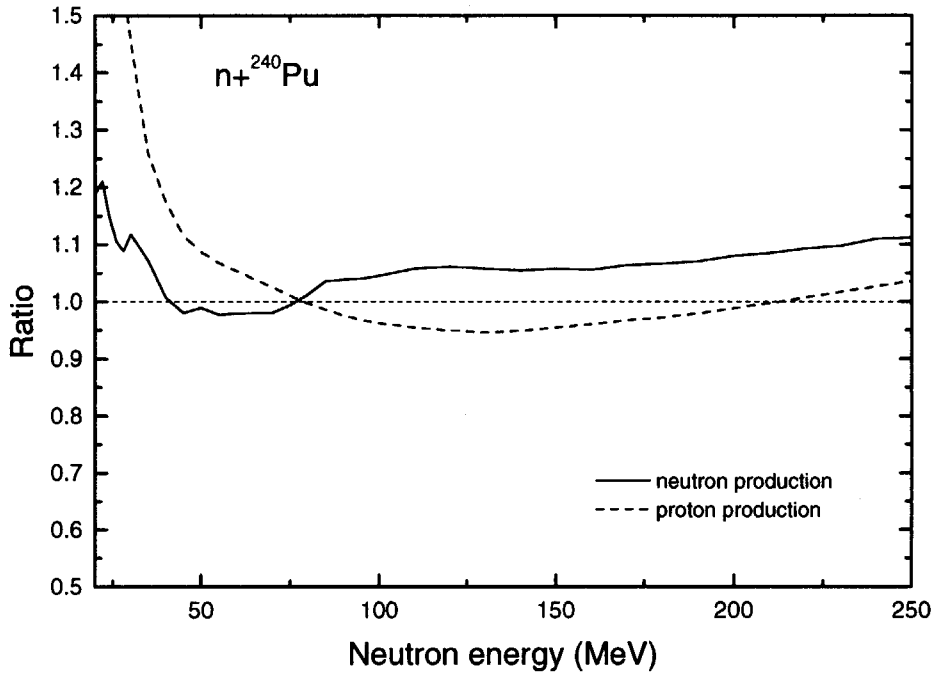

Fig.30 The ratio of the neutron and proton production cross sections calculated by ALICE/ASH code to results obtained with GNASH code for ^{240}Pu.

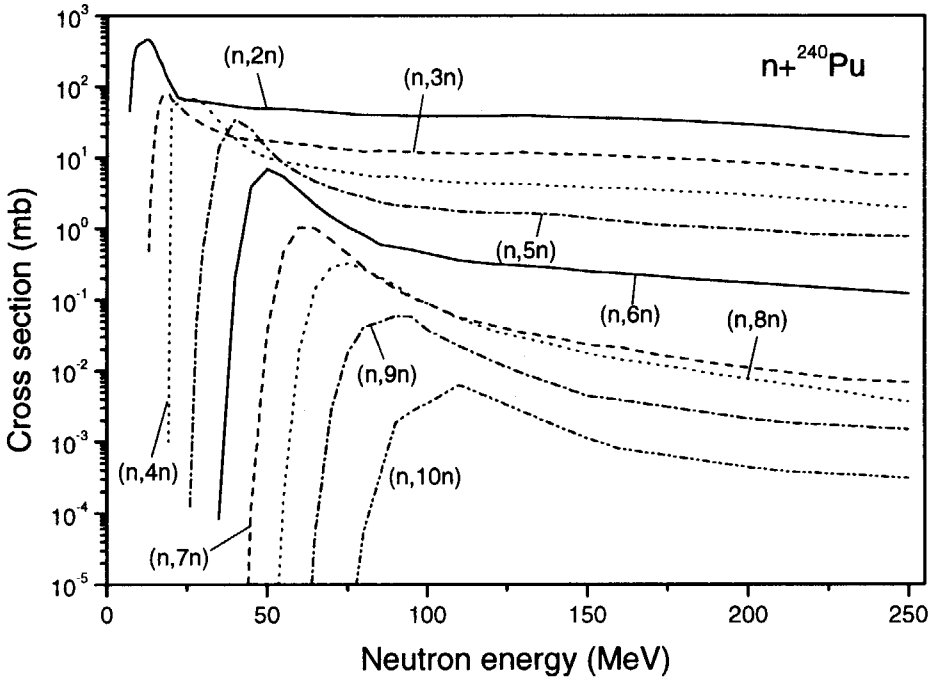

Fig.31 Evaluated (n,xn) reaction cross sections for ^{240}Pu.

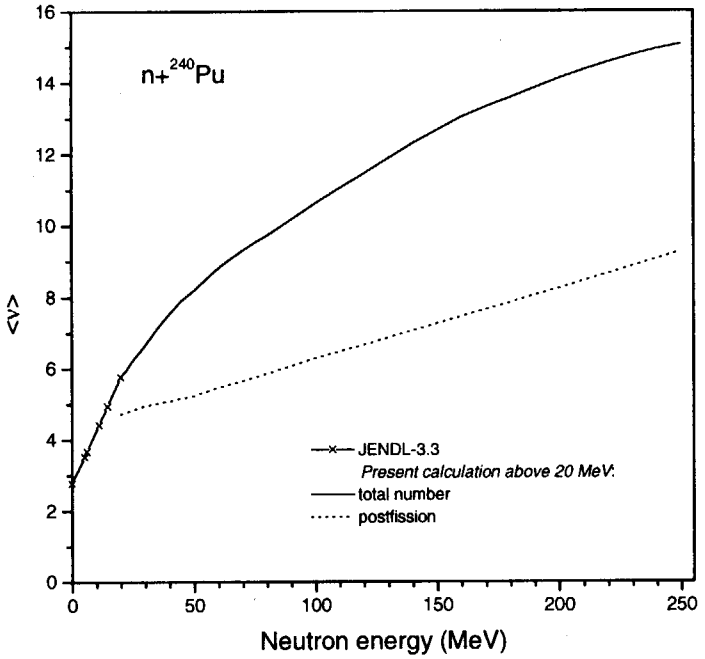

Fig.32 Total number of prompt fission neutrons (solid line) and neutrons emitted from the excited fission fragments (dotted line) evaluated in the present work for ^{240}Pu. Below 20 MeV JENDL-3.3 data (—x—) are shown.

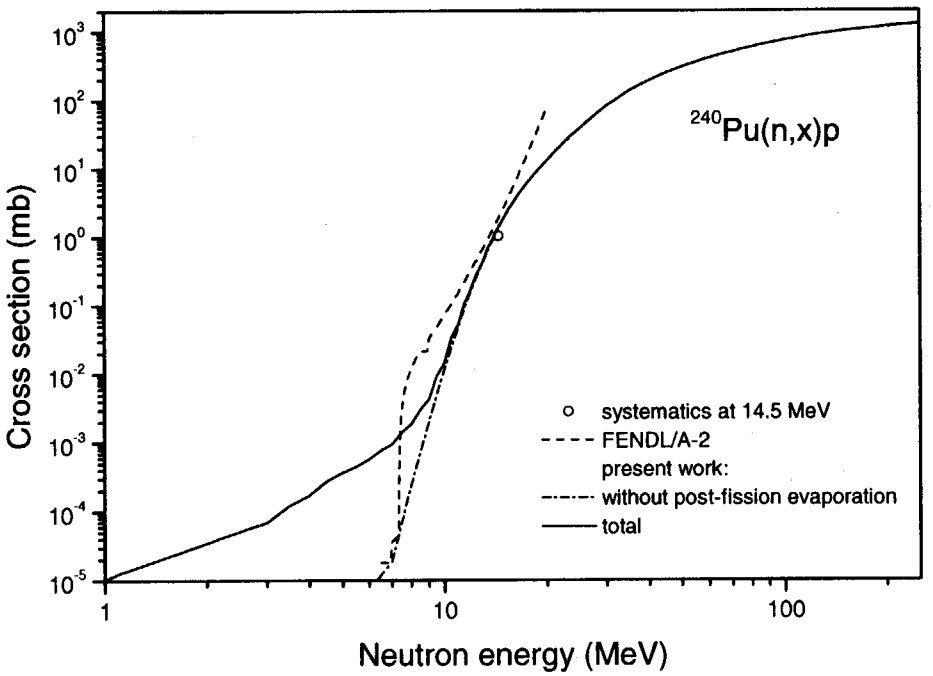

Fig.33 Total proton production cross section for ^{240}Pu, evaluated in the present work, obtained by the systematics [32] and taken from FENDL/A-2.

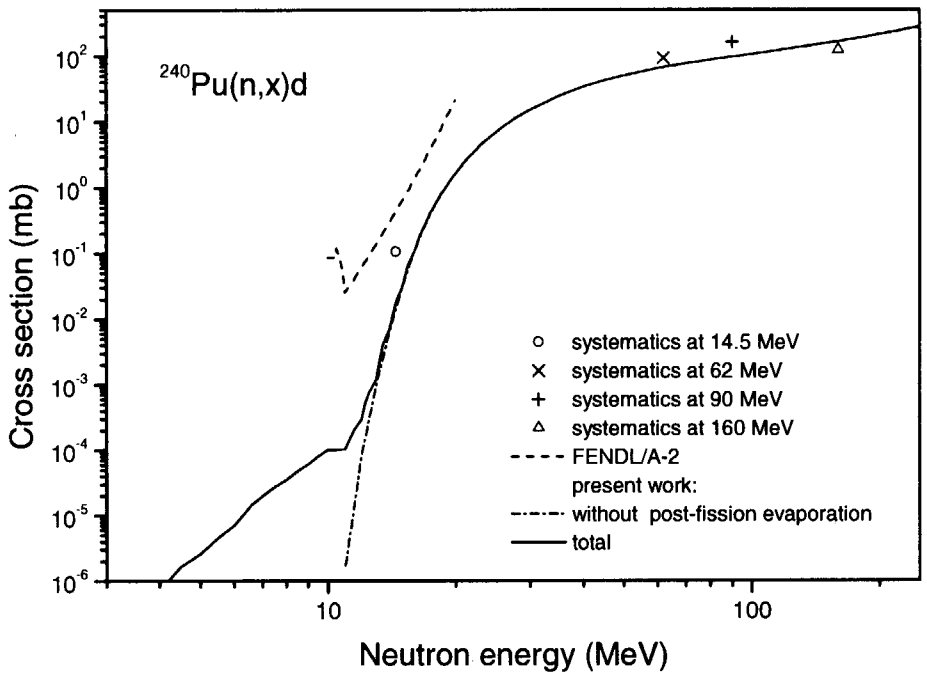

Fig.34 Total deuteron production cross section for ^{240}Pu, evaluated in the present work, obtained by the systematics [5,32] and taken from FENDL/A-2.

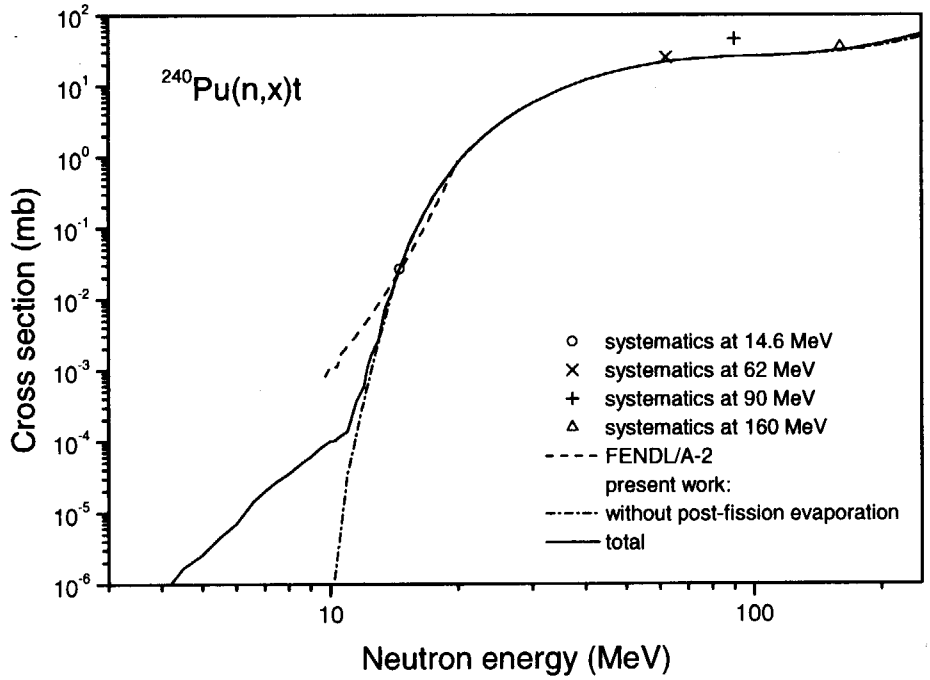

Fig.35 Total triton production cross section for ^{240}Pu, evaluated in the present work, obtained by the systematics [5,32,34] and taken from FENDL/A-2.

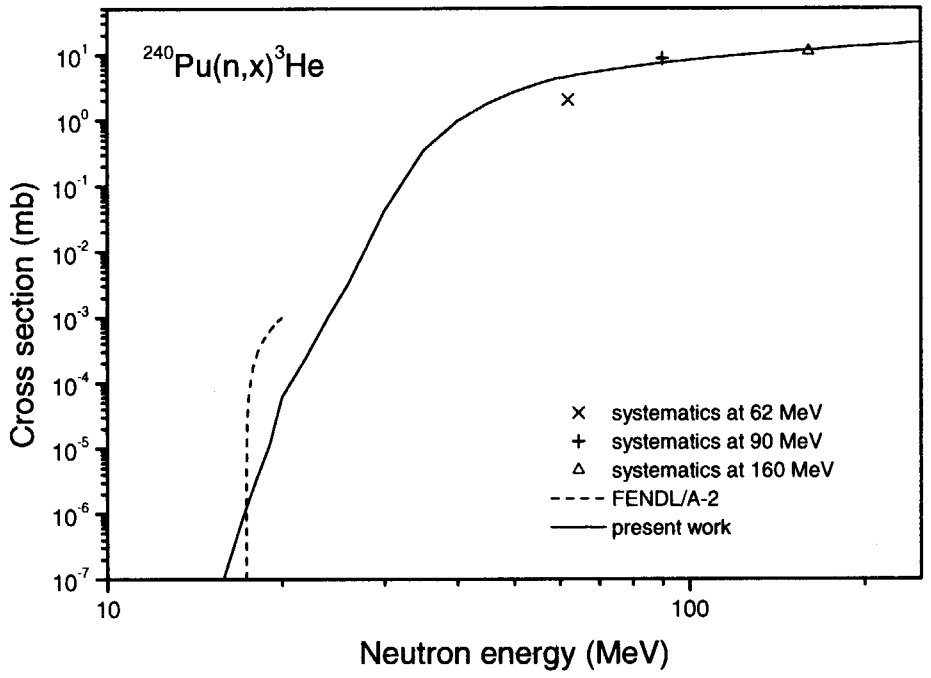

Fig.36 Total ^{3}He-production cross section for ^{240}Pu, evaluated in the present work, obtained by the systematics [5] and taken from FENDL/A-2.

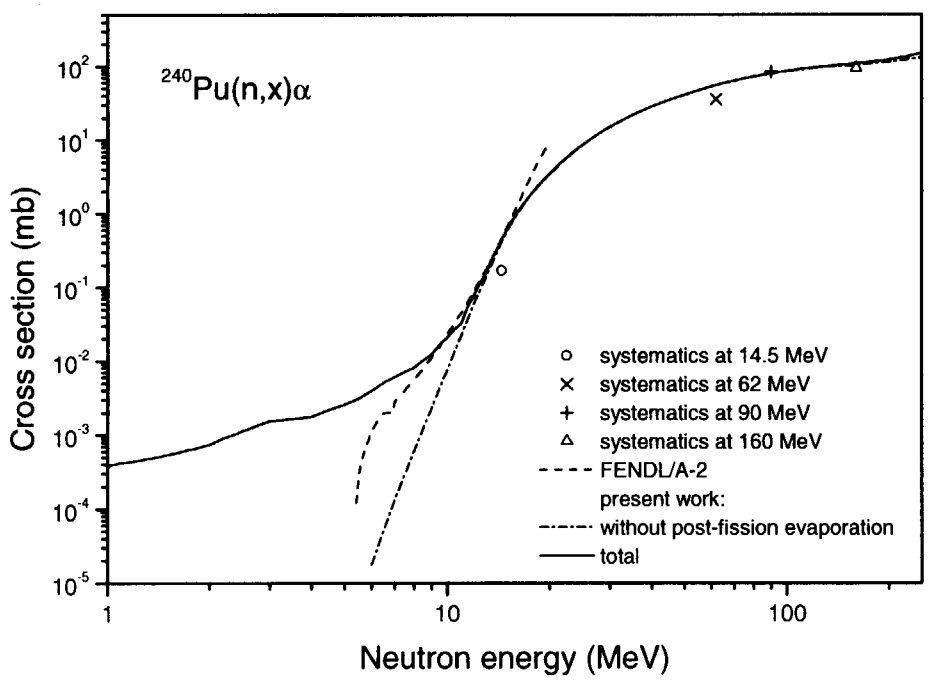

Fig.37 Total α-production cross section for ^{240}Pu, evaluated in the present work, obtained by the systematics [5,32,35] and taken from FENDL/A-2.

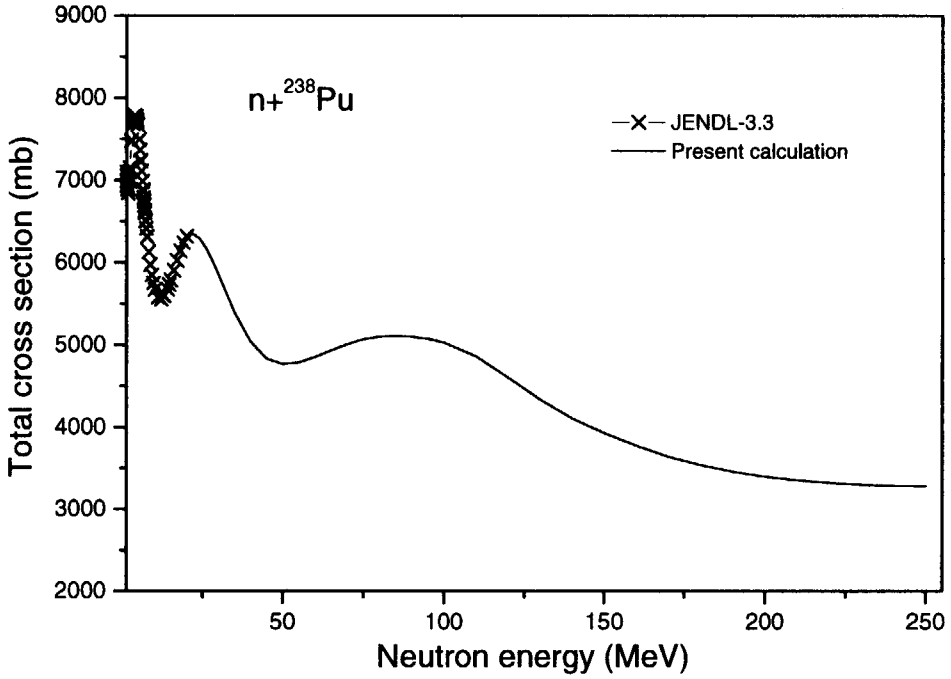

Fig.38 Total neutron cross section for ^{238}Pu obtained in the present work and taken from JENDL-3.3.

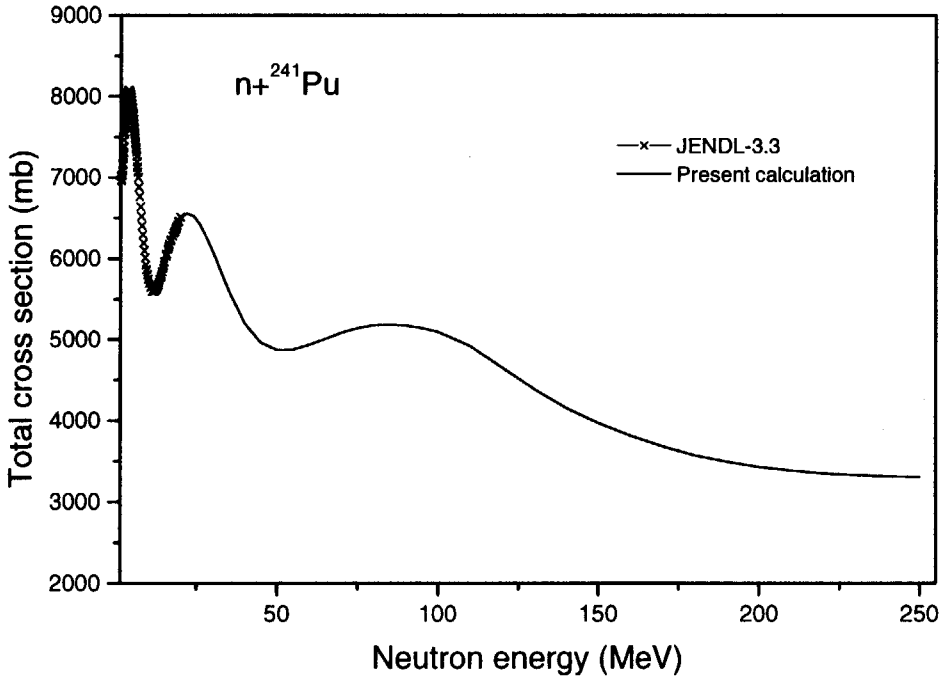

Fig.39 Total neutron cross section for ^{241}Pu obtained in the present work and taken from JENDL-3.3.

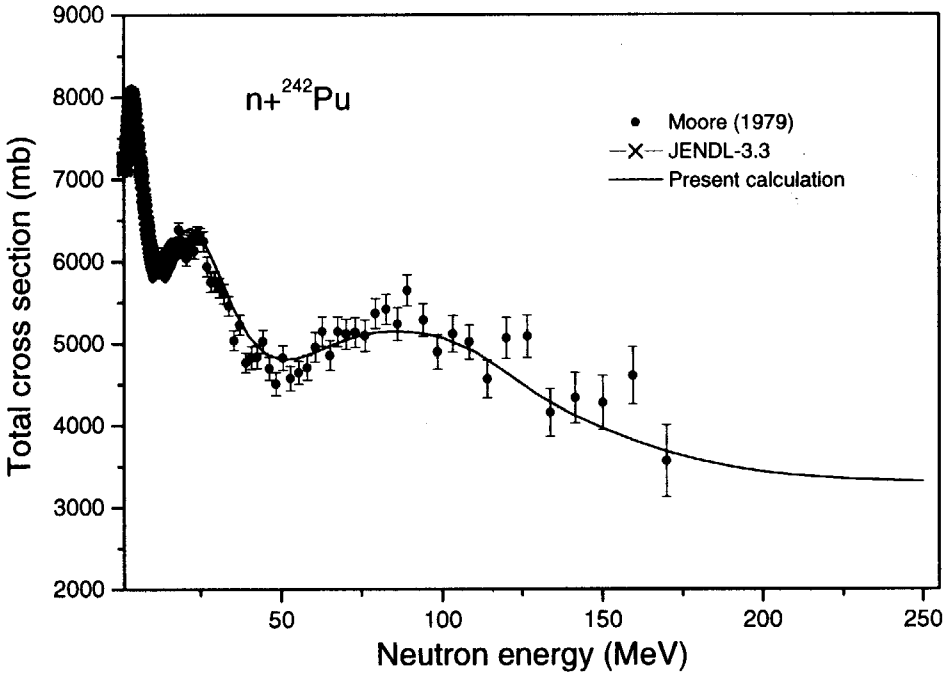

Fig.40 Total neutron cross section for ^{242}Pu obtained in the present work, taken from JENDL-3.3 and measured in Ref.[37].

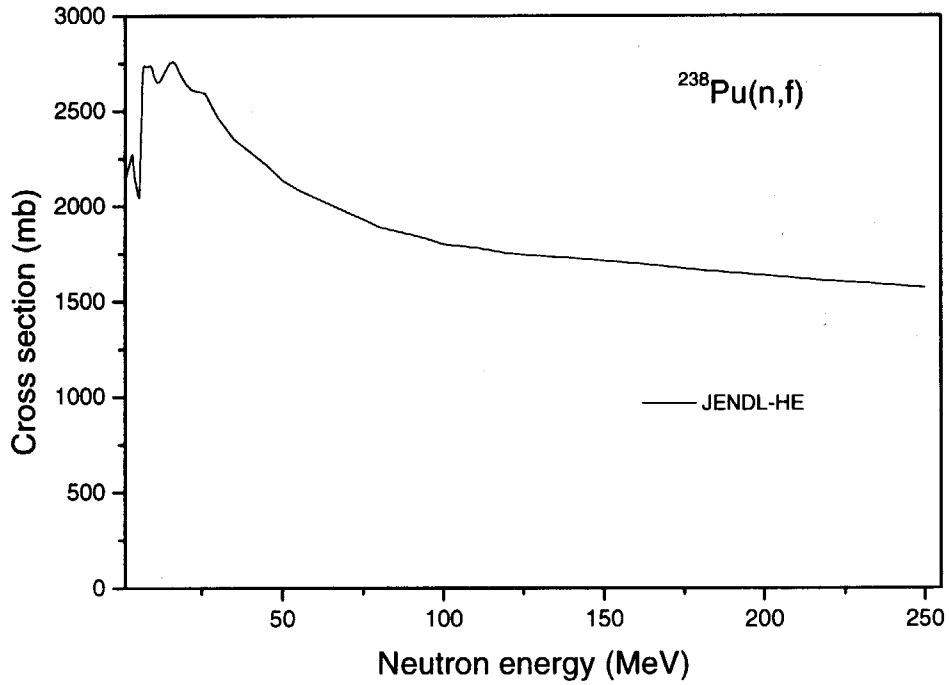

Fig.41 Recommended fission cross section for ^{238}Pu.

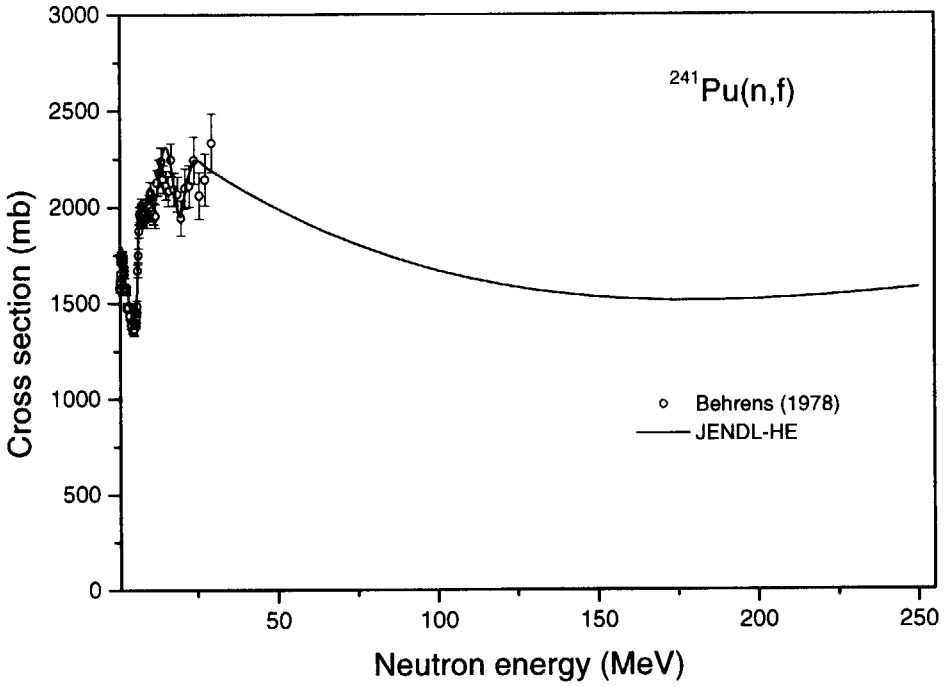

Fig.42 Recommended fission cross section for ^{241}Pu (solid line) and the experimental data from Ref.[38].

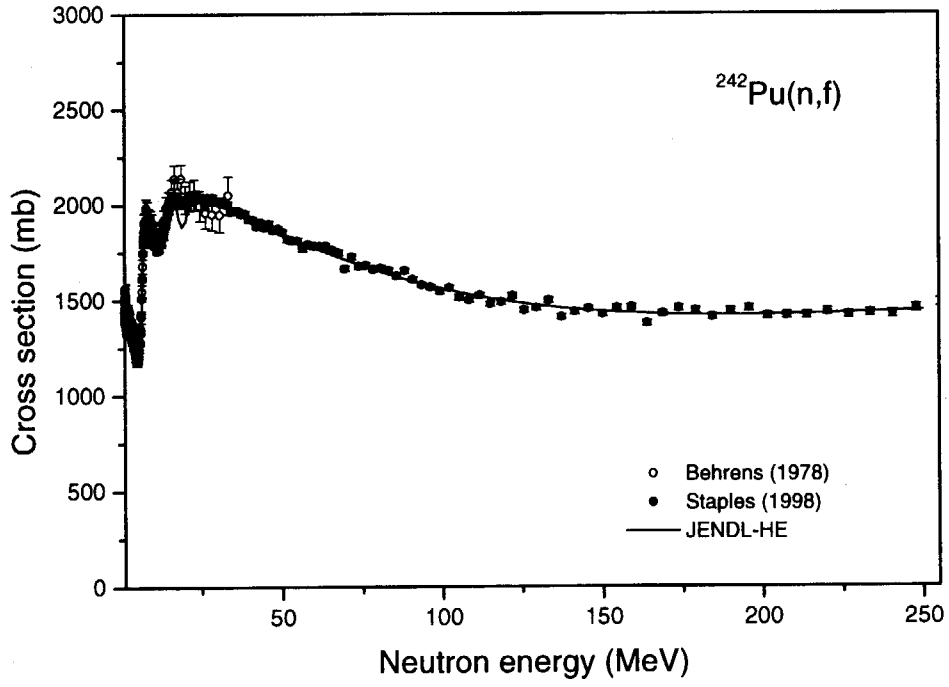

Fig.43 Recommended fission cross section for ^{242}Pu (solid line) and the experimental data from Refs.[28,36].

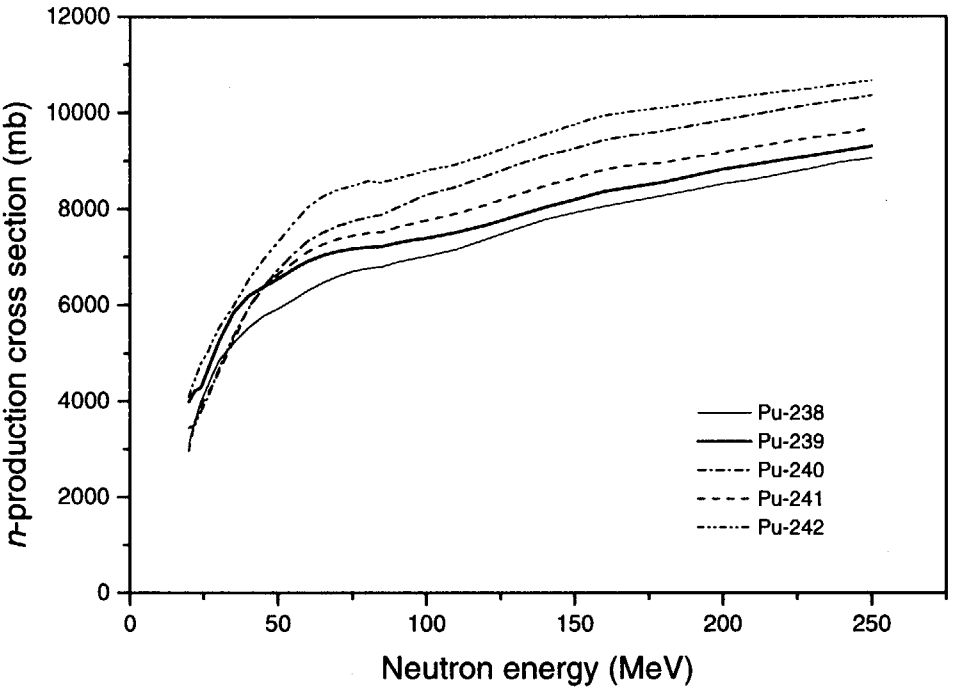

Fig.44 Neutron production cross sections for different plutonium isotopes. The data include the yield of neutrons before the fission and from (n,xnypzα) reactions.

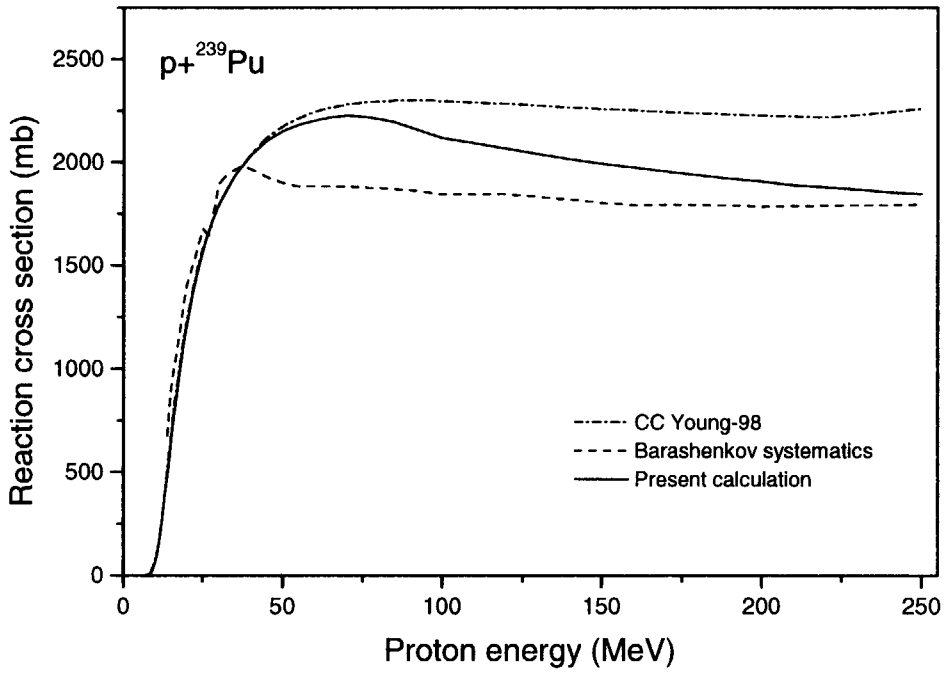

Fig.45 Proton reaction cross section for ^{239}Pu calculated in the present work with the recommended parameters of the optical potential [5] (solid line) and with the parameters from Ref.[20] (dashed-dotted line), the cross sections estimated by the systematics from Refs.[21,22] (dashed line).

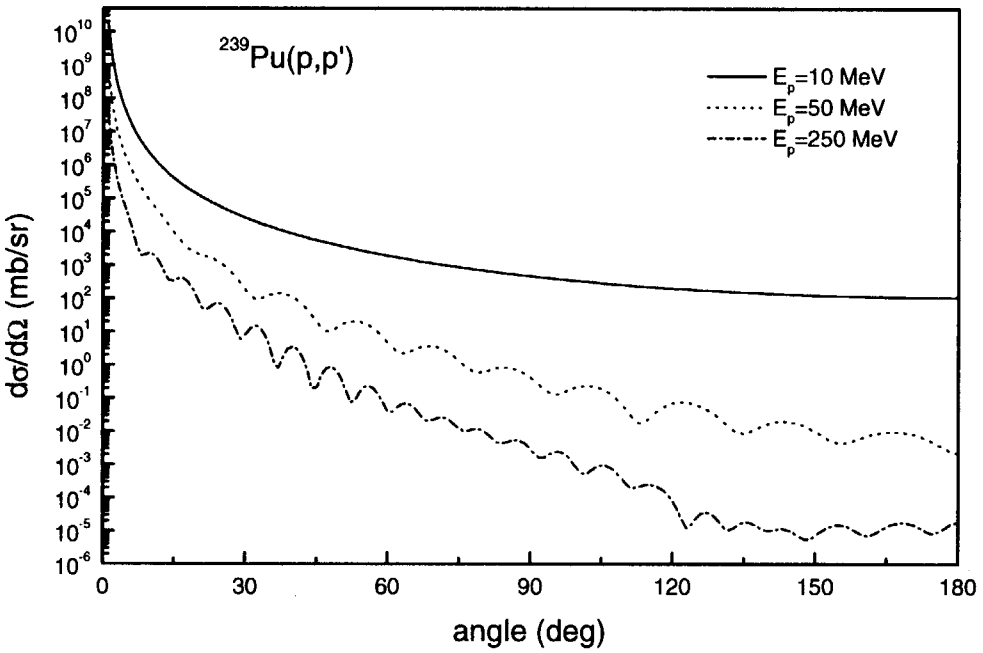

Fig.46 Proton elastic scattering angular distributions calculated in the present work at the different primary proton energies.

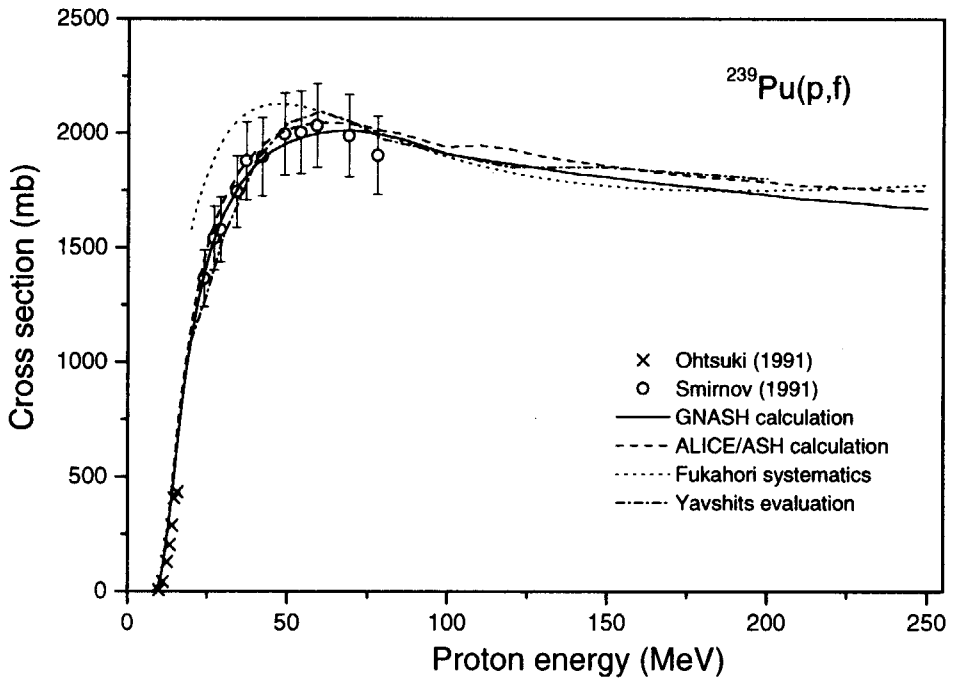

Fig.47 Fission cross section for p+^{239}Pu interaction calculated with GNASH code and ALICE/ASH code, cross section estimated by the systematics [23], data evaluated in Ref.[30] and measured in Refs.[42,43].

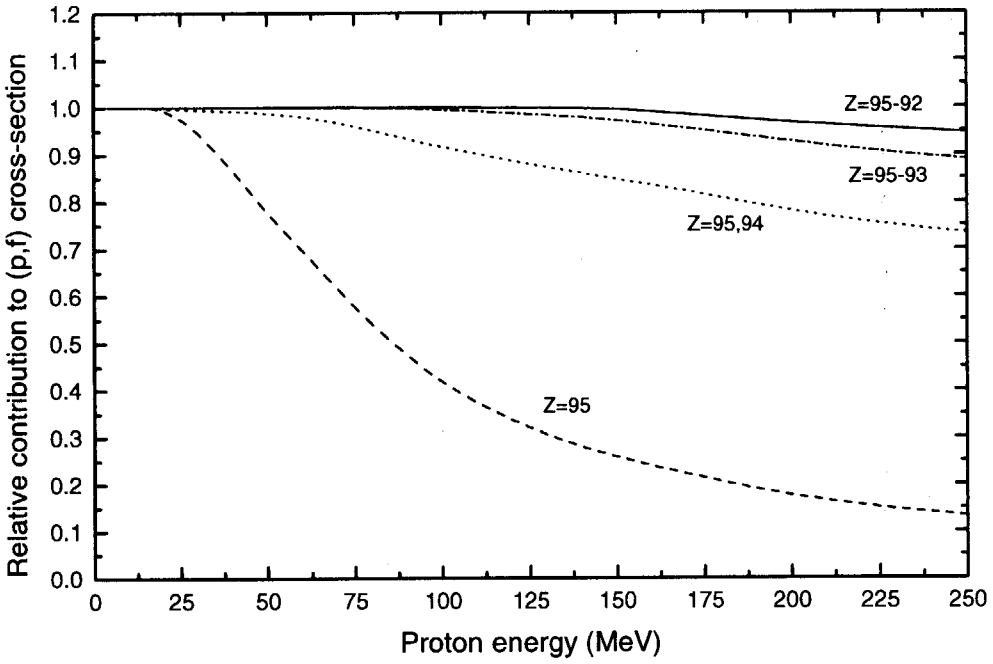

Fig.48 The relative contribution of the nuclei with the different atomic number in the total fission cross section for ^{239}Pu irradiated by protons calculated by GNASH code.

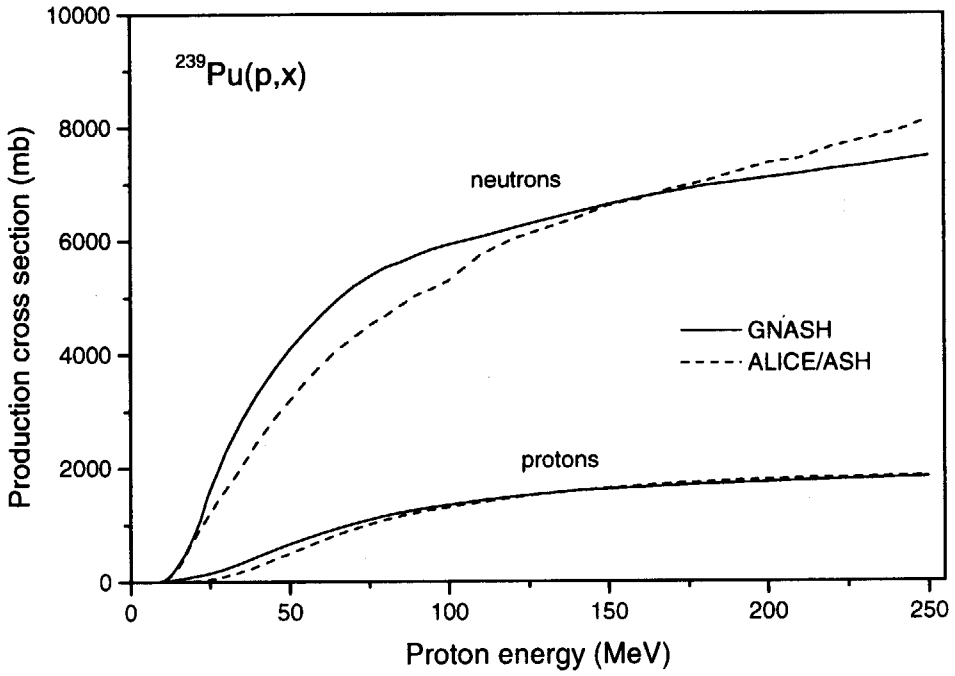

Fig.49 The neutron and proton production cross sections calculated with GNASH code and ALICE/ASH code without the post-fission evaporation contribution.

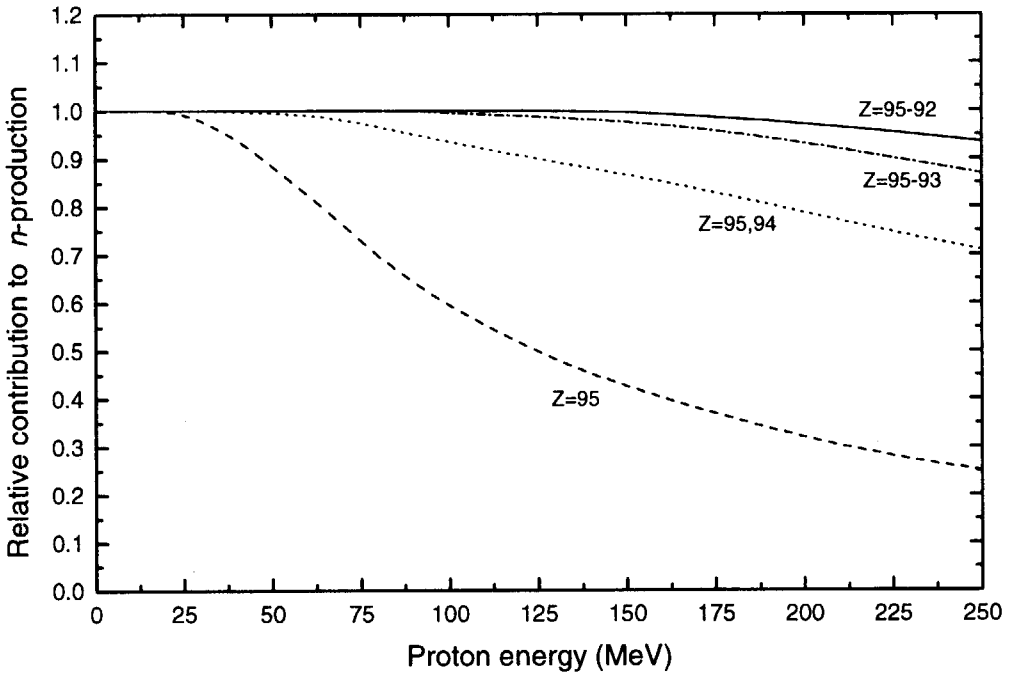

Fig.50 The relative contribution of the nuclei with the different atomic number in the neutron production cross section for p+^{239}Pu interaction calculated by GNASH code. The prompt fission neutrons are not included.

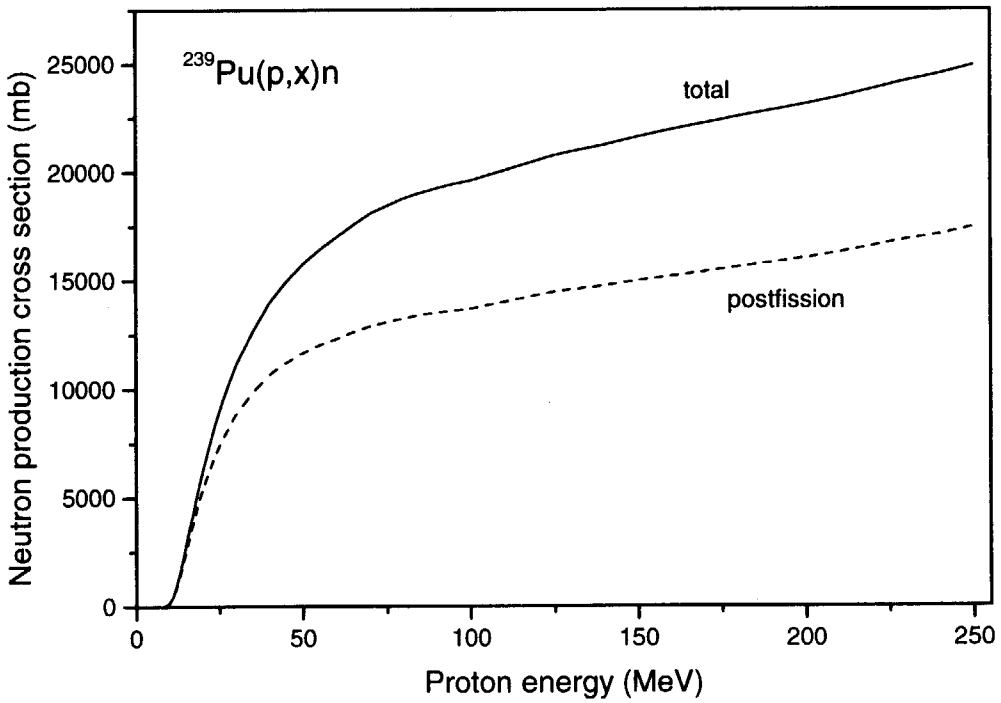

Fig.51 The total neutron production cross section for ^{239}Pu including the contribution from (n,xnypzα) reactions, pre- and post-fission events (solid line), the part of this cross section corresponding to the post-fission evaporation (dashed line).

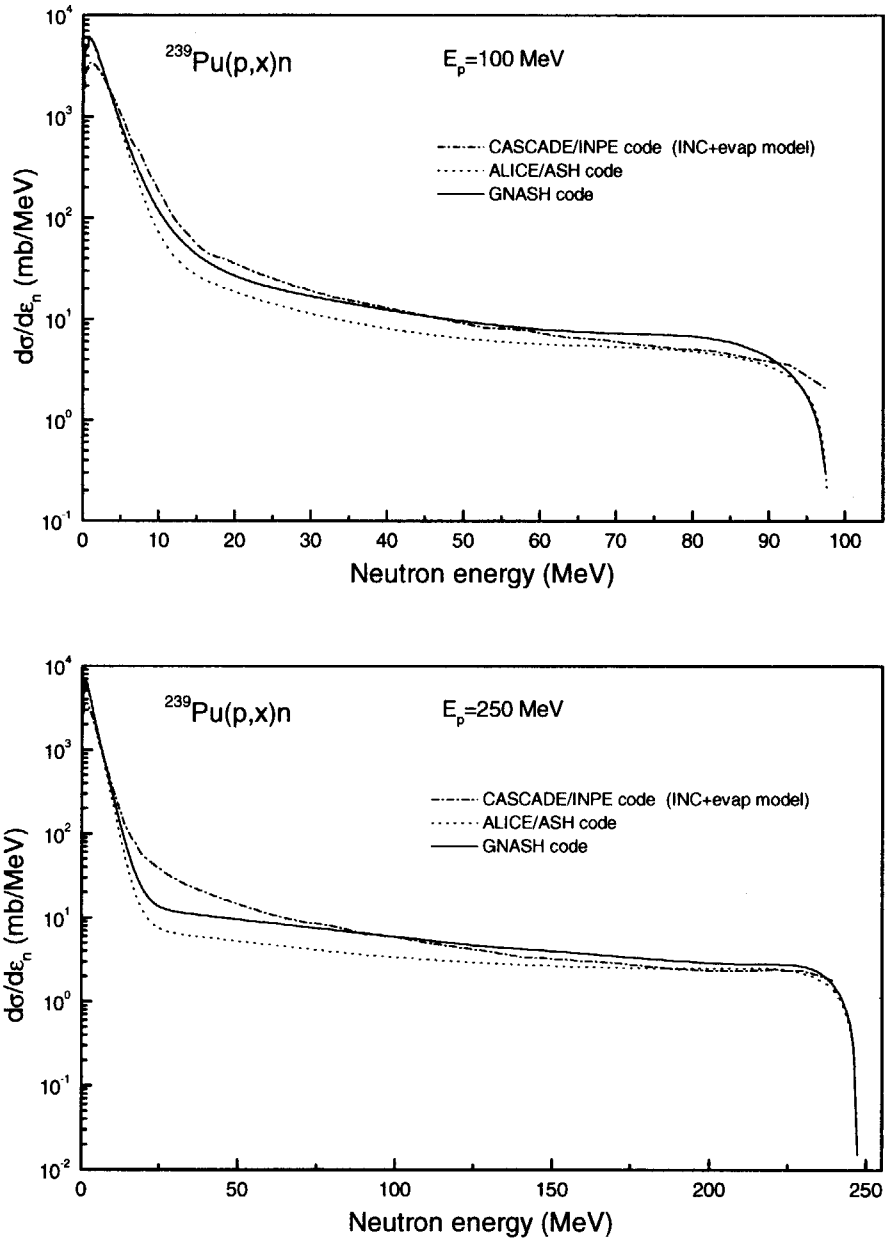

Fig.52 Neutron spectra for ^{239}Pu irradiated by protons, calculated in the present work using GNASH code, ALICE/ASH code and the CASCADE/INPE code.

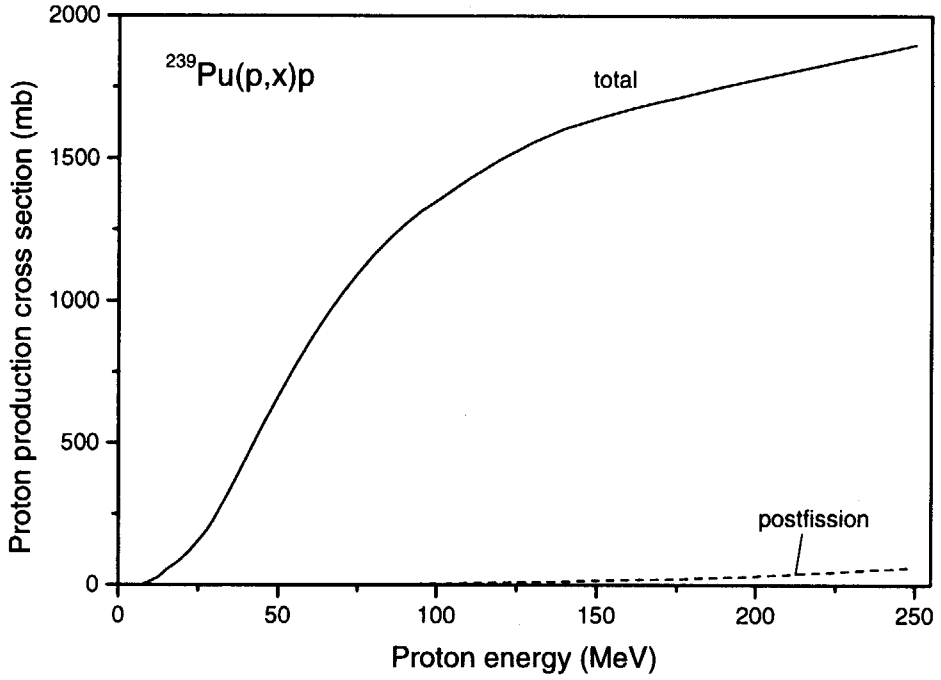

Fig.53 The total proton production cross section for ^{239}Pu including the contribution from (n,xnypzα) reactions, pre- and post-fission events (solid line), the part of this cross section corresponding to the post-fission evaporation (dashed line).

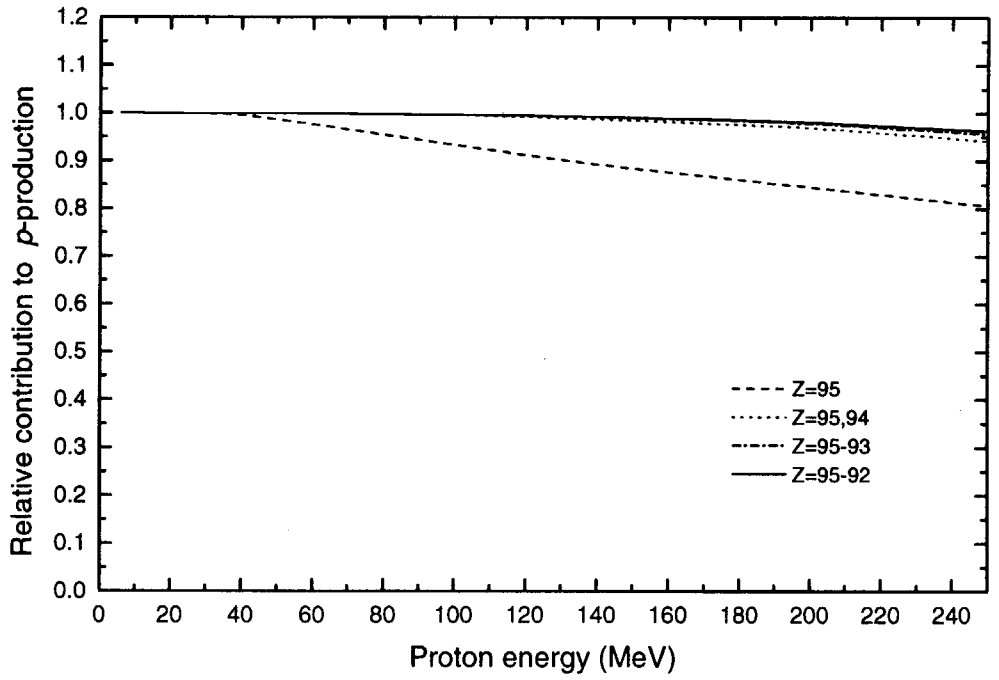

Fig.54 The relative contribution of the nuclei with the different atomic number in the total proton production cross section for p+^{239}Pu interaction.

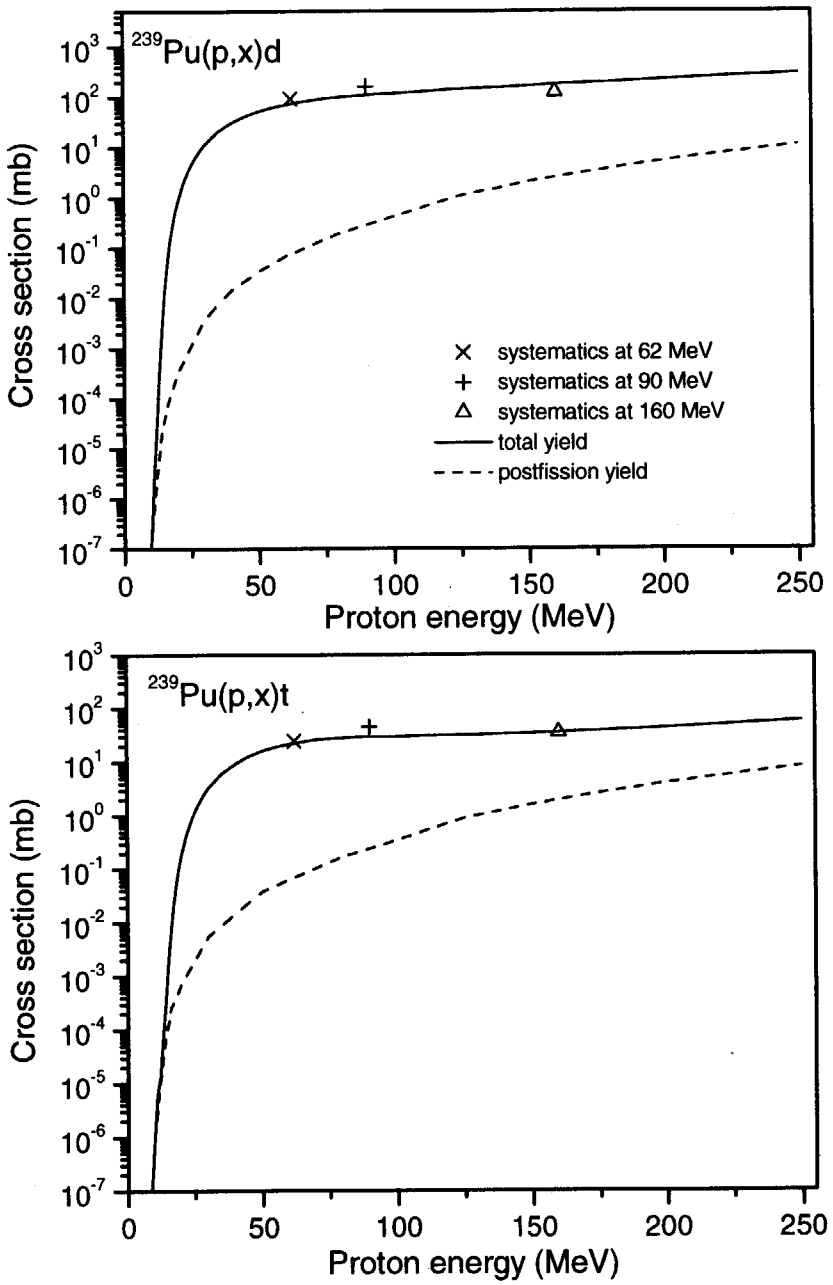

Fig.55 Total deuteron and triton production cross section for ^{239}Pu irradiated by protons (solid line) together with the post-fission contribution (dashed line) obtained in the present work and the cross section estimated by the systematics [5].

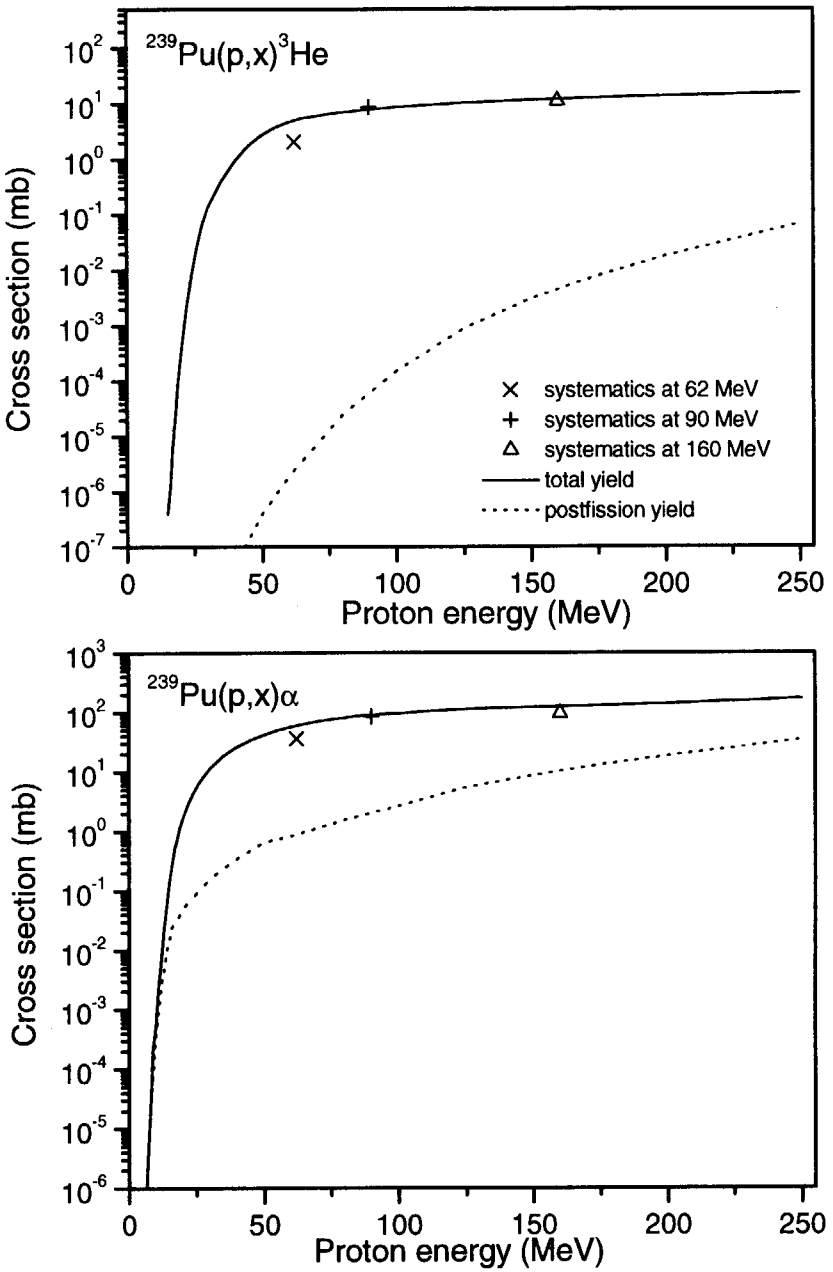

Fig.56 Total ^{3}He- and α-production cross section for ^{239}Pu irradiated by protons (solid line) together with the post-fission contribution (dashed line) obtained in the present work and the cross section estimated by the systematics [5].

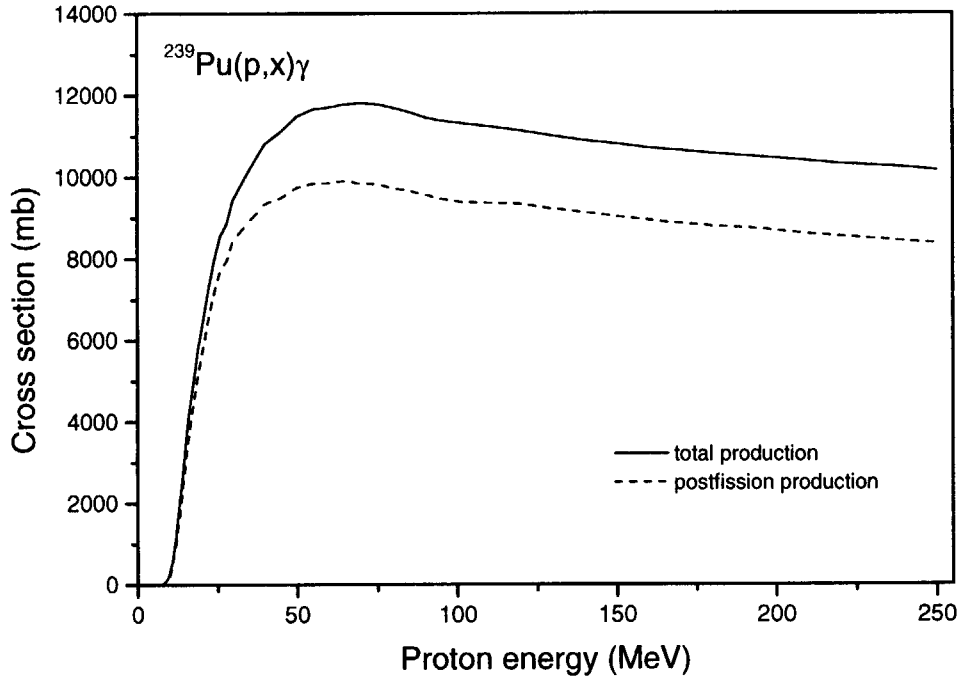

Fig.57 Total γ-production cross section for p+^{239}Pu interaction and the contribution of the post-fission γ-yield.

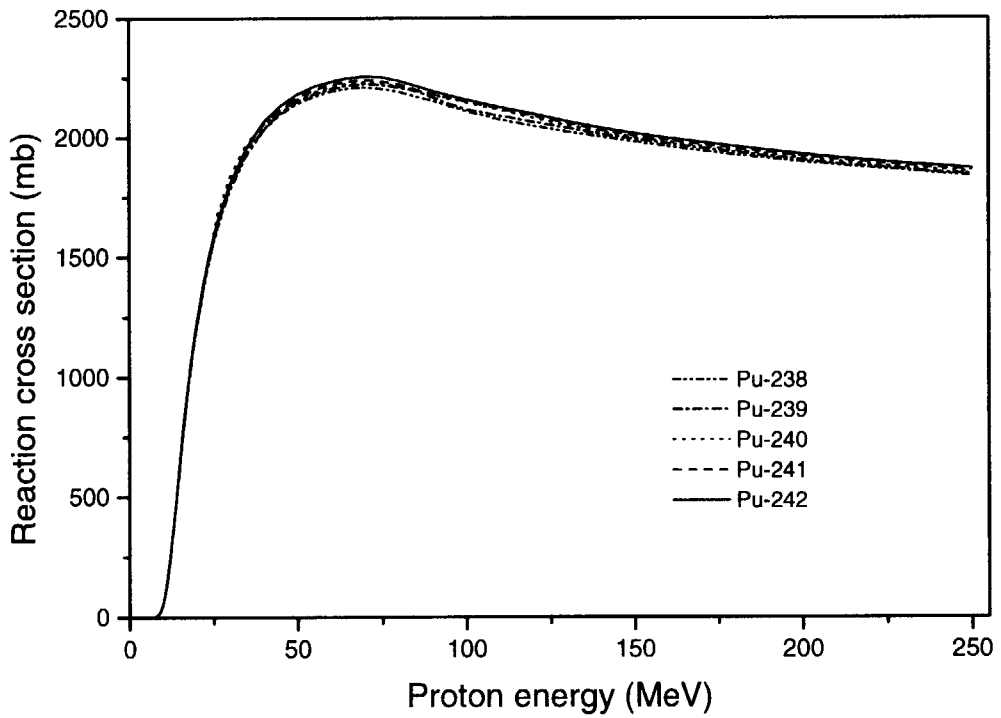

Fig.58 Evaluated proton reaction cross sections for different plutonium isotopes.

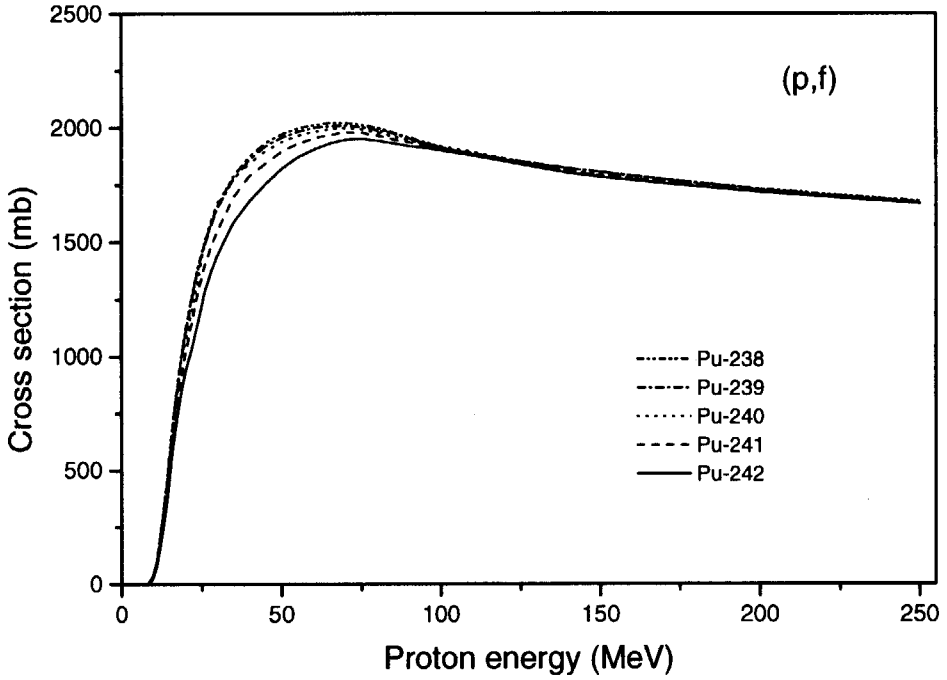

Fig.59 Evaluated proton induced fission reaction cross sections for different plutonium isotopes.

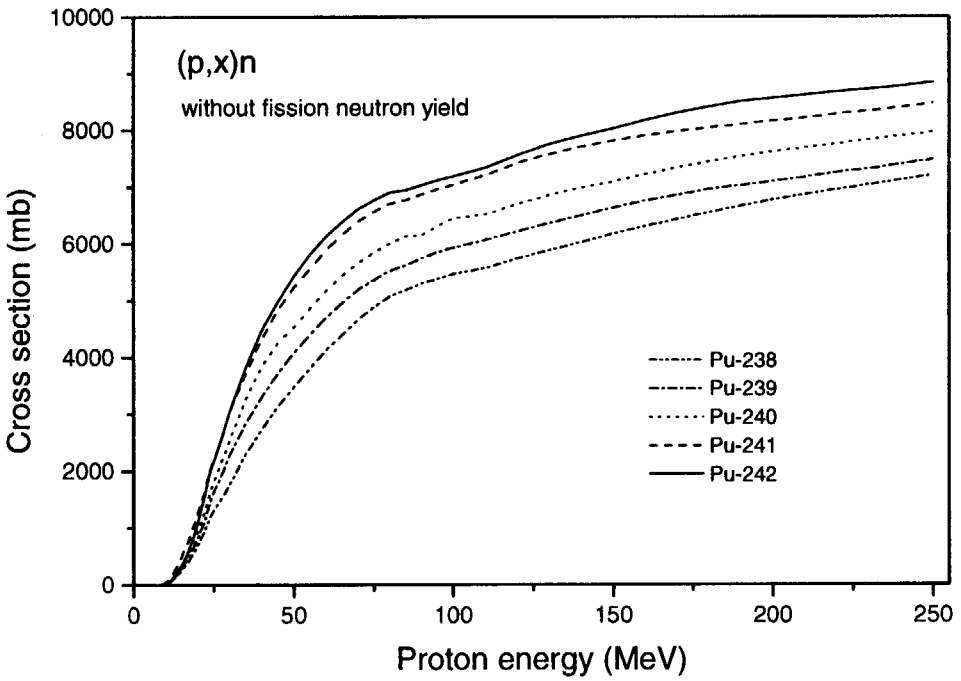

Fig.60 Neutron production cross section including the neutron yield from (p,xnypzα) reactions and pre-fission contribution for different plutonium isotopes irradiated by protons.

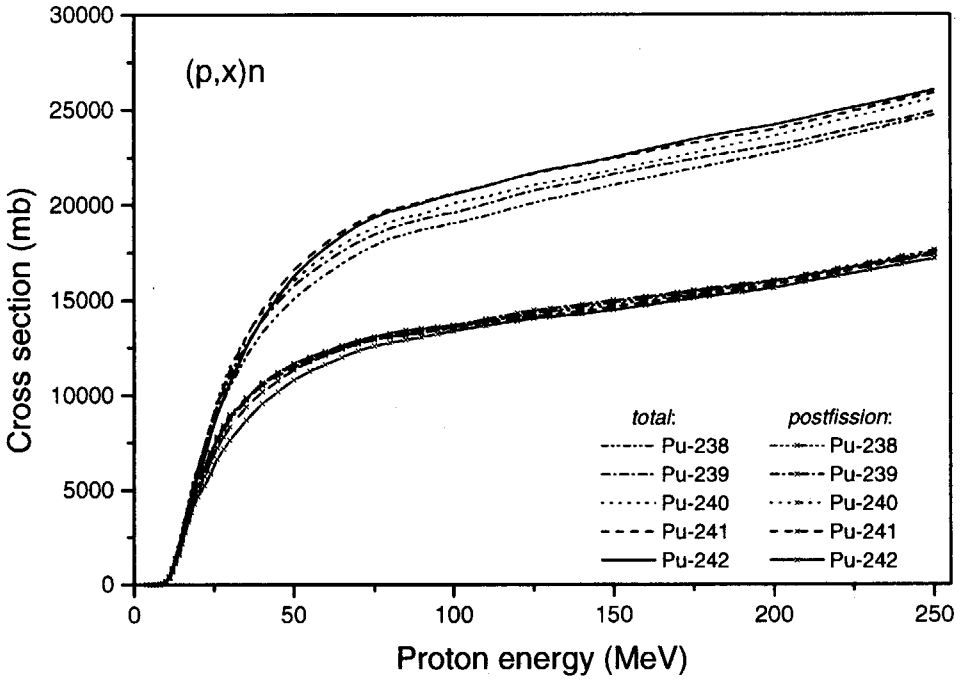

Fig.61 Total neutron production cross section and the post-fission yield contribution for different plutonium isotopes irradiated by protons.

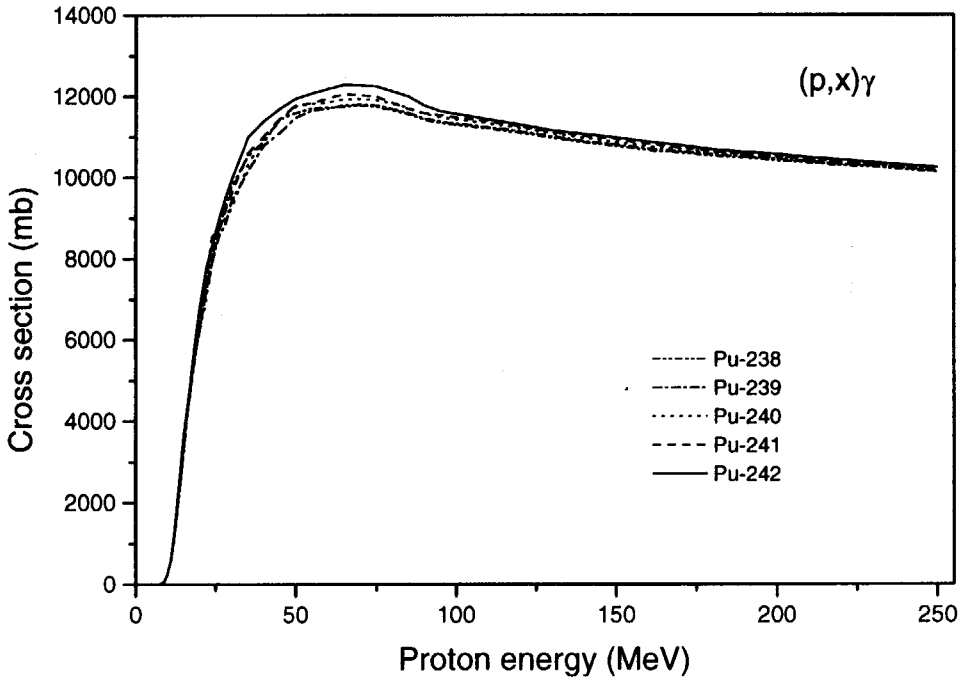

Fig.62 Total γ-production cross section for different plutonium isotopes irradiated by protons.

国際単位系（SI）と換算表

表1　SI基本単位および補助単位

量	名称	記号
長さ	メートル	m
質量	キログラム	kg
時間	秒	s
電流	アンペア	A
熱力学温度	ケルビン	K
物質量	モル	mol
光度	カンデラ	cd
平面角	ラジアン	rad
立体角	ステラジアン	sr

表2　SIと併用される単位

名称	記号
分，時，日	min，h，d
度，分，秒	°，′，″
リットル	l，L
トン	t
電子ボルト	eV
原子質量単位	u

1 eV=1.60218×10^{-19}J

1 u=1.66054×10^{-27}kg

表3　固有の名称をもつSI組立単位

量	名称	記号	他のSI単位による表現
周波数	ヘルツ	Hz	s^{-1}
力	ニュートン	N	$m\cdot kg/s^2$
圧力，応力	パスカル	Pa	N/m^2
エネルギー，仕事，熱量	ジュール	J	N·m
工率，放射束	ワット	W	J/s
電気量，電荷	クーロン	C	A·s
電位，電圧，起電力	ボルト	V	W/A
静電容量	ファラド	F	C/V
電気抵抗	オーム	Ω	V/A
コンダクタンス	ジーメンス	S	A/V
磁束	ウェーバ	Wb	V·s
磁束密度	テスラ	T	Wb/m^2
インダクタンス	ヘンリー	H	Wb/A
セルシウス温度	セルシウス度	℃	
光束	ルーメン	lm	cd·sr
照度	ルクス	lx	lm/m^2
放射能	ベクレル	Bq	s^{-1}
吸収線量	グレイ	Gy	J/kg
線量等量	シーベルト	Sv	J/kg

表4　SIと共に暫定的に維持される単位

名称	記号
オングストローム	Å
バーン	b
バール	bar
ガル	Gal
キュリー	Ci
レントゲン	R
ラド	rad
レム	rem

1 Å=0.1nm=10^{-10}m

1 b=100fm^2=10^{-28}m^2

1 bar=0.1MPa=10^{5}Pa

1 Gal=1cm/s^2=10^{-2}m/s^2

1 Ci=3.7×10^{10}Bq

1 R=2.58×10^{-4}C/kg

1 rad=1cGy=10^{-2}Gy

1 rem=1cSv=10^{-2}Sv

表5　SI接頭語

倍数	接頭語	記号
10^{18}	エクサ	E
10^{15}	ペタ	P
10^{12}	テラ	T
10^{9}	ギガ	G
10^{6}	メガ	M
10^{3}	キロ	k
10^{2}	ヘクト	h
10^{1}	デカ	da
10^{-1}	デシ	d
10^{-2}	センチ	c
10^{-3}	ミリ	m
10^{-6}	マイクロ	μ
10^{-9}	ナノ	n
10^{-12}	ピコ	p
10^{-15}	フェムト	f
10^{-18}	アト	a

（注）

1．表1－5は「国際単位系」第5版，国際度量衡局1985年刊行による。ただし，1 eVおよび1 uの値はCODATAの1986年推奨値によった。

2．表4には海里，ノット，アール，ヘクタールも含まれているが日常の単位なのでここでは省略した。

3．barは，JISでは流体の圧力を表わす場合に限り表2のカテゴリーに分類されている。

4．EC閣僚理事会指令ではbar，barnおよび「血圧の単位」mmHgを表2のカテゴリーに入れている。

換算表

力

N(=10^{5}dyn)	kgf	lbf
1	0.101972	0.224809
9.80665	1	2.20462
4.44822	0.453592	1

粘度　1 Pa·s(N·s/m^2)=10 P(ポアズ)(g/(cm·s))

動粘度　1 m^2/s=10^{4}St(ストークス)(cm^2/s)

圧力

MPa(=10bar)	kgf/cm^2	atm	mmHg(Torr)	lbf/in^2(psi)
1	10.1972	9.86923	7.50062×10^3	145.038
0.0980665	1	0.967841	735.559	14.2233
0.101325	1.03323	1	760	14.6959
1.33322×10^{-4}	1.35951×10^{-3}	1.31579×10^{-3}	1	1.93368×10^{-2}
6.89476×10^{-3}	7.03070×10^{-2}	6.80460×10^{-2}	51.7149	1

エネルギー・仕事・熱量

J(=10^7 erg)	kgf·m	kW·h	cal(計量法)	Btu	ft·lbf	eV
1	0.101972	2.77778×10^{-7}	0.238889	9.47813×10^{-4}	0.737562	6.24150×10^{18}
9.80665	1	2.72407×10^{-6}	2.34270	9.29487×10^{-3}	7.23301	6.12082×10^{19}
3.6×10^6	3.67098×10^5	1	8.59999×10^5	3412.13	2.65522×10^6	2.24694×10^{25}
4.18605	0.426858	1.16279×10^{-6}	1	3.96759×10^{-3}	3.08747	2.61272×10^{19}
1055.06	107.586	2.93072×10^{-4}	252.042	1	778.172	6.58515×10^{21}
1.35582	0.138255	3.76616×10^{-7}	0.323890	1.28506×10^{-3}	1	8.46233×10^{18}
1.60218×10^{-19}	1.63377×10^{-20}	4.45050×10^{-26}	3.82743×10^{-20}	1.51857×10^{-22}	1.18171×10^{-19}	1

1 cal= 4.18605J（計量法）

= 4.184J（熱化学）

= 4.1855J（15℃）

= 4.1868J（国際蒸気表）

仕事率　1 PS(仏馬力)

= 75 kgf·m/s

= 735.499W

放射能

Bq	Ci
1	2.70270×10^{-11}
3.7×10^{10}	1

吸収線量

Gy	rad
1	100
0.01	1

照射線量

C/kg	R
1	3876
2.58×10^{-4}	1

線量当量

Sv	rem
1	100
0.01	1

（86年12月26日現在）

Nuclear Data Evaluation for ^{238}Pu, ^{239}Pu, ^{240}Pu, ^{241}Pu and ^{242}Pu Irradiated by Neutrons and Protons at the Energies up to 250 MeV